NANOPETROPHYSICS CHARACTERIZATION OF THE BAKKEN FORMATION, WILLISTON BASIN, NORTH DAKOTA, USA

by

JOSEPH IKECHUKWU ANYANWU

Presented to the Faculty of the Graduate School of
The University of Texas at Arlington in Partial Fulfillment
of the Requirements
for the Degree of

MASTER OF SCIENCE IN GEOLOGY

THE UNIVERSITY OF TEXAS AT ARLINGTON

May 2015

Acknowledgements

First of all, I want to give God thanks for His grace, mercy and blessings upon my life.

I want to say thank you to my supervisor, Dr. Max Qinhong Hu, for his guidance and support throughout this research project and to my other committee members, Dr. John Wickham and Dr. Ashley Griffith for their support throughout the project.

I would like to thank Julie LeFever and the staffs of the Wilson M. Laird Core and Sample Library and the North Dakota Geological Survey for allowing me to use their facilities, photographs, and samples.

I would like to thank some members of Center for Collaborative Characterization of Porous Media (C3PM) in the persons of Troy Barber, Shawn Yuxiang, Kibria Md Golam, Chris Torres and Douglas Tebo, for their help during the tests used in this project.

Finally, I would like to thank my parents and siblings for their unconditional love and support throughout the period of my education. Special thanks to Donald Madukwe and Louis Ogbeifun for their support and encouragement.

April 3, 2015

Abstract

NANOPETROPHYSICS CHARACTERIZATION OF THE BAKKEN FORMATION, WILLISTON BASIN, NORTH DAKOTA, USA

Joseph Anyanwu, M.S

The University of Texas at Arlington, 2015

Supervising Professor: Max Quinhong Hu

The recent oil boom in the US has been attributed to the result of hydraulic fracturing and horizontal drilling of shale plays. However despite this boom, production and maximum recovery is still limited to be only few percentage of the original oil in place. There have been many studies attempting to enhance the oil recovery of the Bakken Shale, however one area that has not been addressed is the structure of the nanopores storing and transporting the hydrocarbons. The pore geometry and connectivity of these nanopore structures affect the fluid flow and mass transport, which is linked to overall oil recovery.

This work focuses on the connectivity of the nanopore structure within the Bakken shale using cores of all three Bakken members obtained from a producing well in North Dakota. For these tight rock samples, we study pore structure and edge-accessible porosity, using the following complementary tests: 1) mercury injection capillary pressure (MICP); 2) fluid and tracer imbibition into initially-dry sample; and 3) tracer diffusion into fluid-saturated sample. Tracer

imbibition and diffusion is measured by elemental laser ablation-ICP-MS mapping.

Results from the MICP show that the Bakken members have nano-sized pores with low permeability and tortuous flow pathways. Low connectivity of small pore produce anomalous imbibition behavior indicated by the imbibition slope, which is consistent with percolation theory. Limited connected pathways for the tracers were also observed from tracer imbibition and saturated diffusion tests.

The findings from these innovative approaches provide information on pore structure and connectivity that can be used in fluid dynamics to estimate overall oil recovery.

Table of Contents

List of Illustrations

List of Tables

Chapter 1

Introduction

1.1 Overview

Shale oil reservoir developments are a growing source of natural oil and gas reserves across the United States and North America at large. However, they cannot be produced at commercial flow rates without the successful application of some special recovery processes. This is because the shale reservoir rocks are known for their ultra-low permeability. Despite these poor petrophysical properties, shale rocks have proven to be an excellent source of oil and gas, capable of producing at commercial rates, when completed with hydraulically fractured horizontal wells. The Bakken-Three Forks Formations of the Williston Basin have been proven to have high recoverable oil at 7.4billion barrels (USGS, 2013) while the North Dakota Department of Mineral Resources reported a production of 26,261,633 bbl at 1,132,331 bbl per day as of August 2014 (https://www.dmr.nd.gov/oilgas/stats/statisticsvw.asp). This made Bakken petroleum system one of the biggest discoveries and an important unconventional play in the US petroleum system, with production hitting several billions of barrels from several counties of North Dakota and Montana. However, despite producing large barrels of oil daily, the North Dakota Bakken play is producing only 7% of the oil in place (Myths of Bakken: Bismarck Tribune Nov 17th 2014) and this has led to several studies on how to improve recovery.

Hydrocarbon production in tight plays is technically challenging. The primary economic challenge facing the industry is the relatively high cost of new

wells, combined with their rapid initial depletion rate and low recovery factor. The rapid production decline requires that new wells be drilled, and old wells re-fractured or re-stimulated, just to maintain production levels. Like every other play, production in the Bakken play tends to decline several months (years) after the first production (Figure 1.1) and we hypothesize that this is due to geology and specifically, the pore structure (geometry and topology) within the matrix.

The Bakken Formation and its petroleum system is comprised of three members: the Upper (shale), Middle (consisting of dolomites, siltstones and sandstones), and the Lower (shale) Members. The Upper and Lower members are organic-rich shale believed to be the source rock, which have expelled oil into the Middle Bakken layer, the target zone of recent hydraulic fracturing.

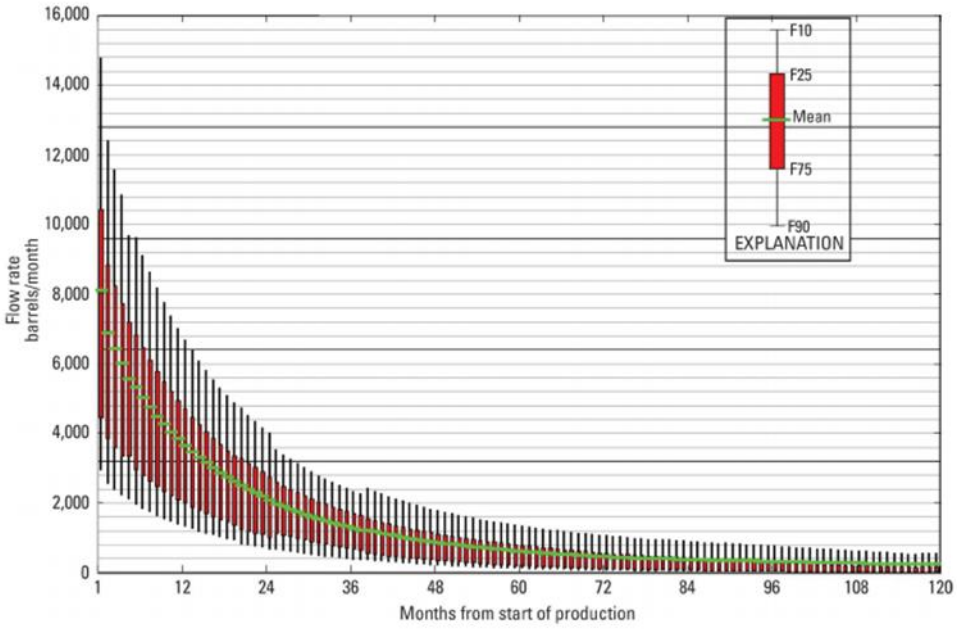

Figure 1-1 Decline curve analysis of Bakken: showing ten-year probabilistic-type curve (PTC) for all horizontal wells in the Bakken Formation and Three Forks Formation (Cook, 2013)

Although, the Middle Bakken is presently the main focus for production with extensive horizontal drilling operations, hydraulic fracturing and development, there has been production from the Upper Shale Member since the late 1970's to the early 1990s around the southwest part of the basin in North Dakota (Lefever et al, 1991). However, recently there has been growing interest in the Upper Bakken and, Sonnenberg (2014) reported that the Upper Shale has recently been targeted with horizontal drilling and multistage fracture stimulations in areas where the Middle Member pinches out. Thus, it becomes interesting to

study the reservoir potentials of the Bakken Shales with respect to pore-throat distribution and connectivity.

1.2 Location of Study Area

The location of the study area is geographically situated in the western part of Stark County in North Dakota. Cores were collected from Kubas well in the Bell oil field located on latitude and longitude of 46.947777N and -103.123496W respectively (Figure 1.2).

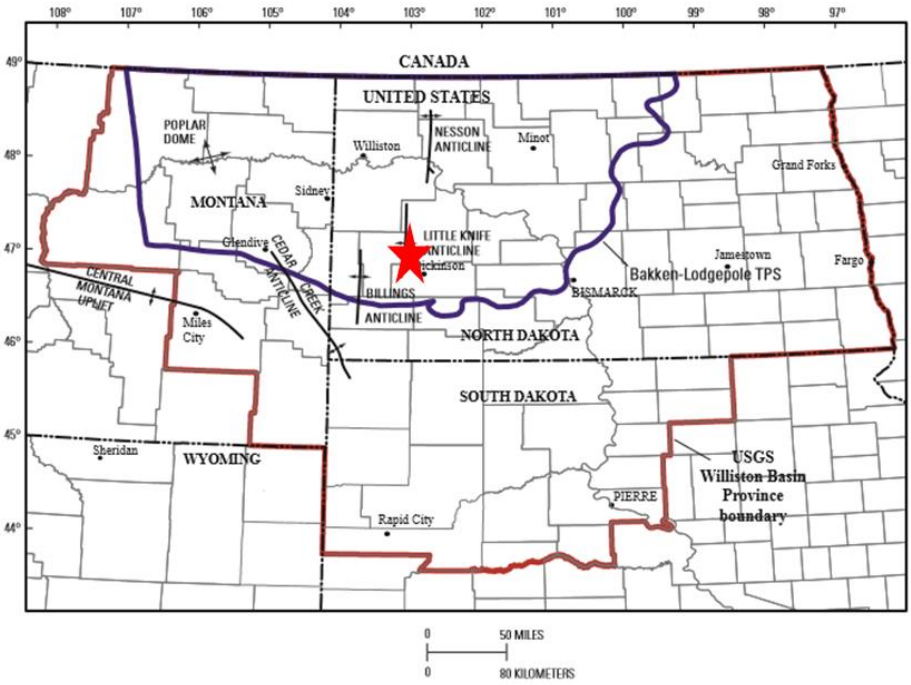

Figure 1-2 United States area extent of the Williston Basin and Bakken Formation, Red star symbol the location of the Bell oil field in Stark County (modified from Pollastro et al., 2010).

1.3 Objectives and Scope of Study

The main objective of this work is to study and characterize the nanopore structure and probe connectivity within the Bakken cores from distribution pattern of tracers in fluid by using complementary laboratory experiments.

As a result of pore structure and low pore connectivity, large amounts of hydrocarbons are left behind during primary production. Hu et al., (2012) reported that fluid flow and solute transport in rock are macroscopic consequences of the pore structure, which integrates geometry (e.g., pore size and shape, pore-size distribution) and topology (e.g., pore connectivity) (Figure 1.3). The pore size distribution, porosity, permeability and natural fracture conduits determine the storativity and transmissibility of oil in the rock matrix, and as such, when pore connectivity is low, topological factors outweigh the better-known geometrical factors (Ewing and Horton, 2002; Hu et al., 2002; Hunt et al., 2014).

Since good pore network provides flow channels for enhanced oil production, the potential prevalence of low pore connectivity in Bakken and other tight plays and its significant impacts on fluid flow and hydrocarbon transport, have generated much interest lately, partly, due to poor documentation and understanding in the past. Hence, this study will help to bridge the gap between pore structure, (with respect to accessibility and connectivity) and dynamic fluid behavior in tight plays, as they affect migration of hydrocarbon molecules from the shale matrix into the stimulated fracture and overall oil recovery.

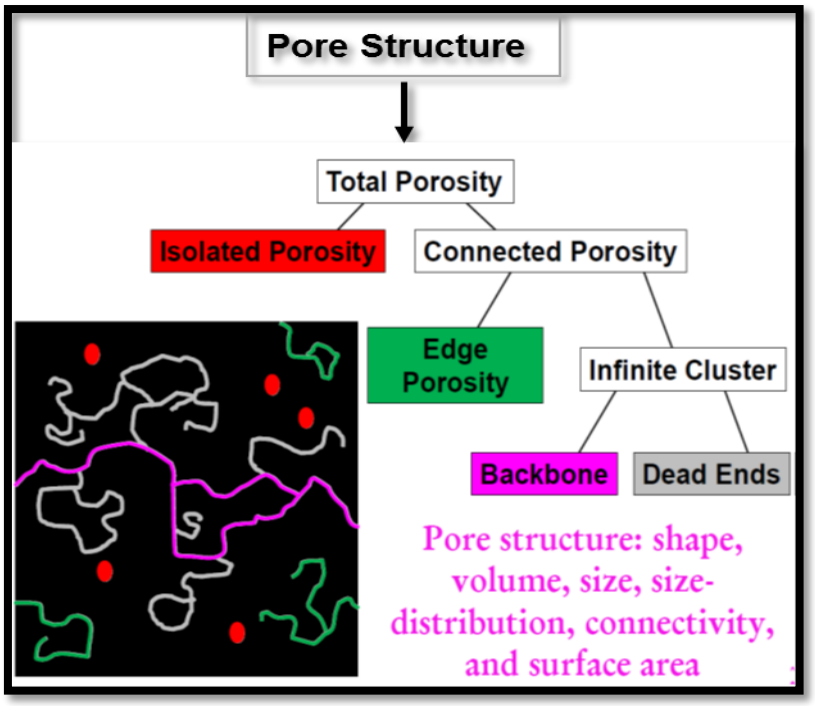

Figure 1-3 Diagrammatic sketch of a pore structure showing distribution of pore throats and shapes with connectivity patterns

1.4 Literature Review and Previous Works on Bakken Formation

The Bakken Petroleum system, widely referred to as a shale play is consist of three members: Upper, Middle and Lower Members. The Upper and Lower Shale Members are organic-rich shales acting as the source from rocks while the Middle Member (silty to dolomitic), feeds from the source rocks, and acts as the reservoir. While the shale members have similar petrophysical properties, the Middle Member has the better reservoir parameters (because it

can be easily fractured due to the brittleness of its rock fabric) needed for production and hence production shifted from the low-producing Upper Shale to the Middle Member during the early 80's and 90's. Even though the Middle Member is the center of attention for most production in the Williston Basin, commercial production and development activities have only become increasingly viable in recent years due to advances in horizontal drilling and use of multi-stage fracture stimulation.

The Bakken source rocks have TOC values varying from 1wt.% to as high as 35% in the shallower and deeper part of the Williston Basin respectively (Jin and Sonnenberg, 2012) with API gravity of 10-55 °API (Heck et al., 1999), and viscosity of 36 cp (Tran, 2011). Petrophysical characterization of the Bakken has been challenging with continuous research going on to better understand and improve oil recovery from the reservoirs. Like most shale plays, the Bakken system is characterized by complex petrophysical parameters and as such, optimum oil recovery is dependent on lithology, mineralogy, fluid properties and the types of pores inherent. The most common and important aspects of the complex petrophysical parameters is a function of its porosity and fracture permeability. The fractures are believed to be the primary path of fluid flow within the Bakken petroleum system and thus good understanding of their sizes and distribution within the reservoir matrix cannot be over emphasized. Breit et al.,(1992) commented that most of the fractures are generally vertically oriented thereby making it difficult for vertical wells to connect, resulting in low productivity, while horizontal wells drilled parallel to the Bakken bedding plane

would intersect many such extensional fractures and therefore improve production. Sonnenberg, (2014), reported that the Upper Shale Member serves both as a source rock and also contributes as a reservoir to production, as it has been targeted for horizontal drilling and multistage fracture stimulations along the southwest edge of Elm Coulee Field where the Middle Member pinches out.

In addition to its low permeability, Schuler et al., (2011), reported that the Bakken play has a characteristic of very light oil (API gravity over 40 degrees) residing in an oil-wet or mixed-wet condition. This oil-wet condition makes it difficult for the aqueous phase to penetrate into the matrix and displace the residing oil, thereby limiting enhanced oil recovery from water-flooding. In other words, oil cannot be spontaneously produced from oil-wet rocks except the capillary pressure barrier between fracture conduits and matrix is overcome.

Several authors in the past have used different chemical additives to study imbibition in shales. Olafuyi et al., (2007), demonstrated that spontaneous imbibition can be studied on small core plugs while Wang et al., (2010) reported that API brine and surfactactants formulations can imbibe in shales and displace oil. Standes and Austad (2000) reported that oil was successfully produced via spontaneous imbibition. Thus the study of spontaneous imbibition is important in enhanced oil recovery processes from rock matrix. Fluid flow and solute transport in rock with low pore connectivity can be characterized by percolation theory, the mathematics of flow pathways and scaling in disordered systems (Hu et al., 2012). However, the process of spontaneous imbibition of fluid into any rock matrix is challenging as it depends on factors such as permeability, wettability,

shape, size of the matrix, saturation history, interfacial tension and viscosity of the fluid system (Olafuyi et al., 2007; Tiab and Donaldson, 2012). The decision was made to study pore structure using both water-and oil-wetting fluids enhanced with tracers to study not just the rate of imbibition, but also the connectivity of these pores within the samples.

There are limited publications on the porosity, pore-size distributions and permeability within the Bakken members (Table 1-1). Ramakrishna et al., (2010) estimated the pore throat radius to have R50 value of 0.002 microns, hence the need to study the pore-throat distributions of the three members of the Bakken Formation and their pore structure in general. Table 1-1 summarizes some of the petrophysical parameters reported in the literature.

Table 1-1 Summary of the petrophysical parameters

Rock	Parameters	Average Value	Source
Upper & Lower Shale (source rock)	TOC (wt.%)	1 to 35	Jin and Sonnenberg (2012)
	API Gravity(°API)	19-55	Heck et al. (1999)
	Viscosity (cp)	0.36	Tran (2011)
	Sw (%)	30-60	Tran (2011)
	φ (%)	3.6	Breit et al. (1992), and Kuhn et al. (2012)
	k (mD)	0.01-0.03	Tran (2011)
Middle Member	Matrix φ (%)	3.7-8.0	Pitman et al. (2001)
	Fracture φ (%)	0.02-12.8	Pitman et al. (2001)
	Matrix *k* (mD)	0-0.04	Pitman et al. (2001); Ramakrishna et al. (2010); Kuhn et al. (2012)
	Fracture *k* (mD)	0.6-54.5	Pitman et al. (2001)
	Pore-throat distribution	0.02-0.0272	Ramakrishna et al. (2010)

Chapter 2

Geologic Setting

2.1 Structural History of Williston Basin

The Bakken Formation is located in the Williston Basin of North Dakota, a large, roughly circular intercratonic sedimentary basin located on the North American Craton covering several hundred thousand square miles across parts of North and South Dakota, Montana, and the Canadian provinces of Manitoba and Saskatchewan (Figures 1.2 & 2.1). The basin has a complex tectonic history, and this is due to the deformation of underlying basement rocks and major bounding fault systems. These fault systems are responsible for much of the basin's interior faults and lineaments, block-fault movements, sedimentation patterns, salt dissolution, fluid movement and thermal history (Pollastro et al., 2010).

At the beginning of the Phanerozoic, prior to the supercontinent breakup, production of heat lenses caused a partial melting of the lower crust and upper mantle. This was followed by emplacement of anorogenic granites during extensional tectonics resulting in the supercontinent breakup. Intrusion of anorogenic granites and other partially melted intrusive rocks weakened the continental lithosphere, thus providing a zone of localized regional stretching and permitting the formation of cratonic basins. (Dev and Hsui, 1987). LeFever et al. (1991) reported that North Dakota is underlain by one of the Superior Craton, which is one of the cratons created and emplaced 2.75 - 2.6 billion years ago and consists mainly of granites and greenstones. Anna et al. (2011) and Monahan

(2014) reported that in the Precambrian, the Archean Superior Craton was sutured to the Archean Wyoming Craton by the Trans-Hudson Belt. This resulted in a north-south trending strike-slip fault and shear belt that created zones of weakness that controlled the location of several anticlines in the basin today (Figure 2.2 A-B)**.** A weak zone was developed by the Trans-Hudson Orogenic belt to the west of the basin and led to sagging during the Cambrian, creating the subsequent Williston Basin.

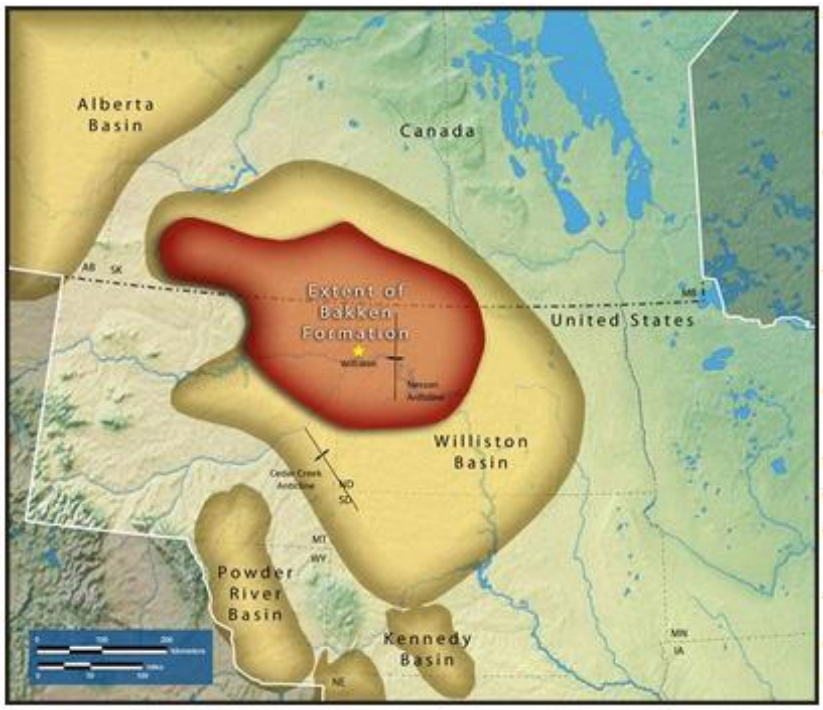

Figure 2-1 Geographical extent of Williston Basin and the Bakken Formation (image source: Energy & Environmental Research Center, 2013, Bakken Formation)

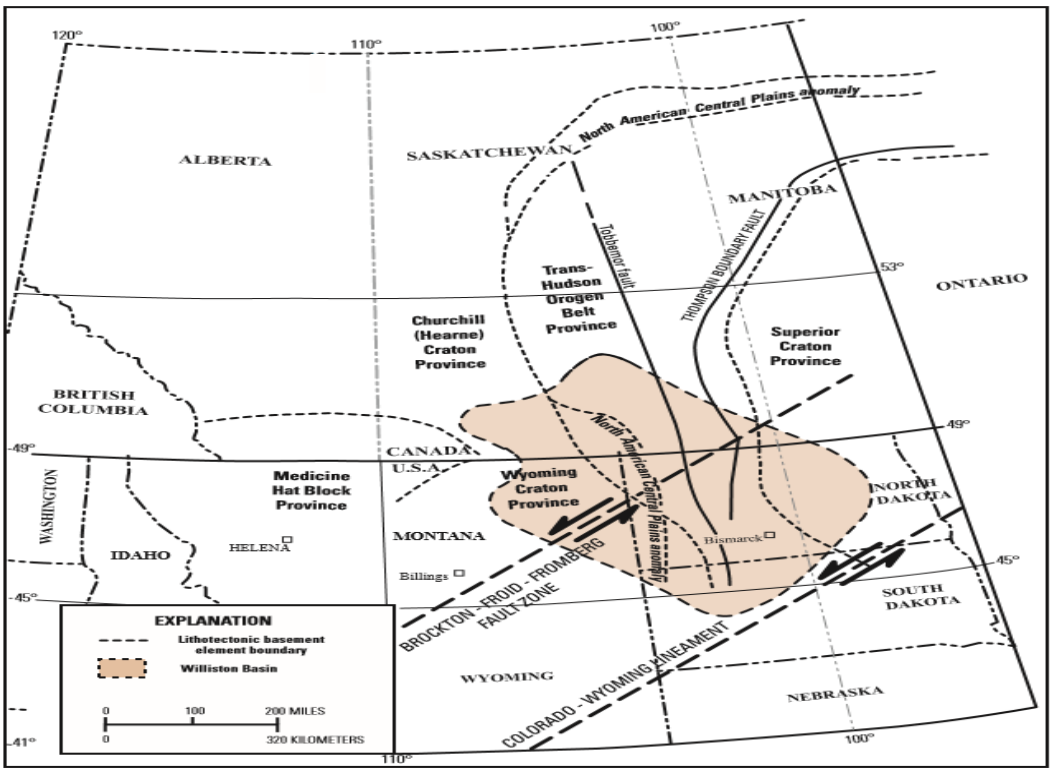

Figure 2-2 General structural extent of the Williston Basin with two major fault systems responsible for the formation of the basin in the Precambrian (Pollastro et al., 2010)

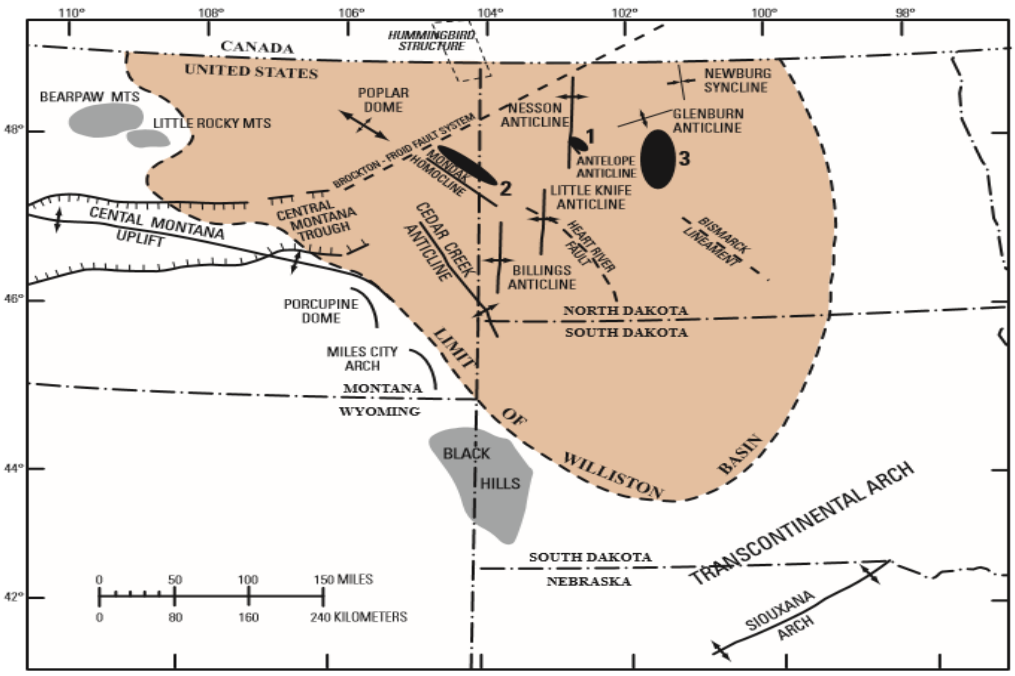

Figure 2-3 Present day major structural elements of the US portion of the Williston Basin. Solid black ovals show general location of major areas of oil production from the Bakken Formation (Pollastro et al., 2010)

2.2 Regional Stratigraphy and Sedimentology of the Williston Basin

The North Dakota portion of the Williston basin has experienced nearly continuous sedimentation with sediments running from the Cambrian through the Tertiary time. The basin sedimentation is characterized by cyclical transgression and regressions with repeated depositional sequence of carbonates and clastics (LeFever et al., 1991). These cycles of sea level change are classified into six major depositional sequences which in ascending order, are the Sauk,

Tippecanoe, Kaskaskia, Absaroka, Zuni, and Tejas, and they account for most of the sedimentary rocks found in the Williston Basin (Sloss, 1963) (Figure 2.3).

The Bakken Formation falls under the Devonian-Mississippian Kaskaskia Sequence that was a result of two transgressive cycles, and as such the sequence is divided into two cycles, with an unconformity that separates the younger Devonian rocks from the older Devonian to form an upper and lower sequence. Rocks of the lower cycle record a northwest connection into the Elk Point Basin while deposition in the upper cycle records a westward connection into the Central Montana Trough (LeFever, 1991).

Deposition of the Upper Kaskaskia Sequence began sometime after middle Lodgepole deposition (Figure 2.4), during the time when the sedimentation in the basin records a change in sediment source from the Elk Point Basin to the Central Montana Trough (LeFever, 1991). Termination by erosion of the Upper Kaskaskia sequence took place approximately during the Mississippian and Pennsylvanian boundary. The rocks of the Absaroka sequence (Pennsylvanian through Triassic) consist mostly of siliciclastic sediments with some evaporites and carbonates present (Simenson, 2010).

The Lower Kaskaskia sequence is a result off transgression from the northwest of the Elk Point Basin, and this resulted in the deposition of the Ashern and Winnipegosis Formations. The Lower Kaskaskia sequence showed repeated cycles and as such is dominated by carbonates with few clastics and evaporates up until the Three Forks Formation. The boundary between the Bakken and Three-Forks Formations marks the boundary between the Upper and Lower

Kaskaskia sequence. Gerhard et al. (1987) and LeFever et al. (1991) reported that the Devonian and Mississippian strata are separated by an unconformity which represents uplift and erosion or sea level change. At this time, the Devonian strata were uplifted and exposed along the basin margin, while deposition continued in the deeper portion of the basin, implying that the Mississippian sediments were later deposited on the eroded Devonian surface.

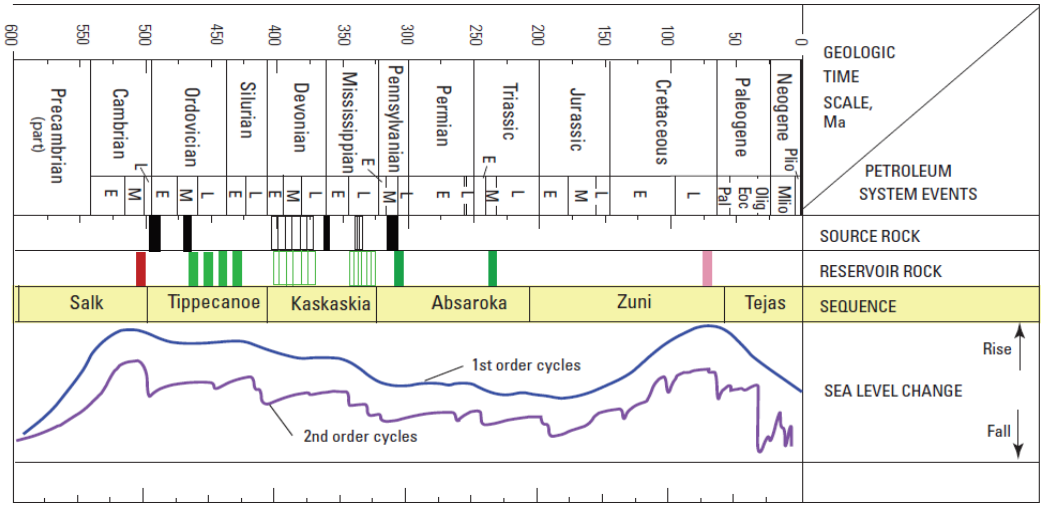

Figure 2-4 Time-stratigraphic column of the Williston Basin with Milankovitch Cycles and Petroleum Plays. Solid black intervals in the source rock column are for thick accumulations; thin lines indicate an association with carbonate depositional cycles. For the reservoir rock column, green is for oil and red for gas; thin lines indicate generalized reservoir rock and do not necessarily represent the full spectrum of possible reservoirs. E, Early; M, Middle; L, Late; Pal, Paleocene; Eoc, Eocene; Olig, Oligocene; Mio, Miocene; Plio, Pliocene (Anna, et al., 2011). Diagram from Anna et al. (2011).

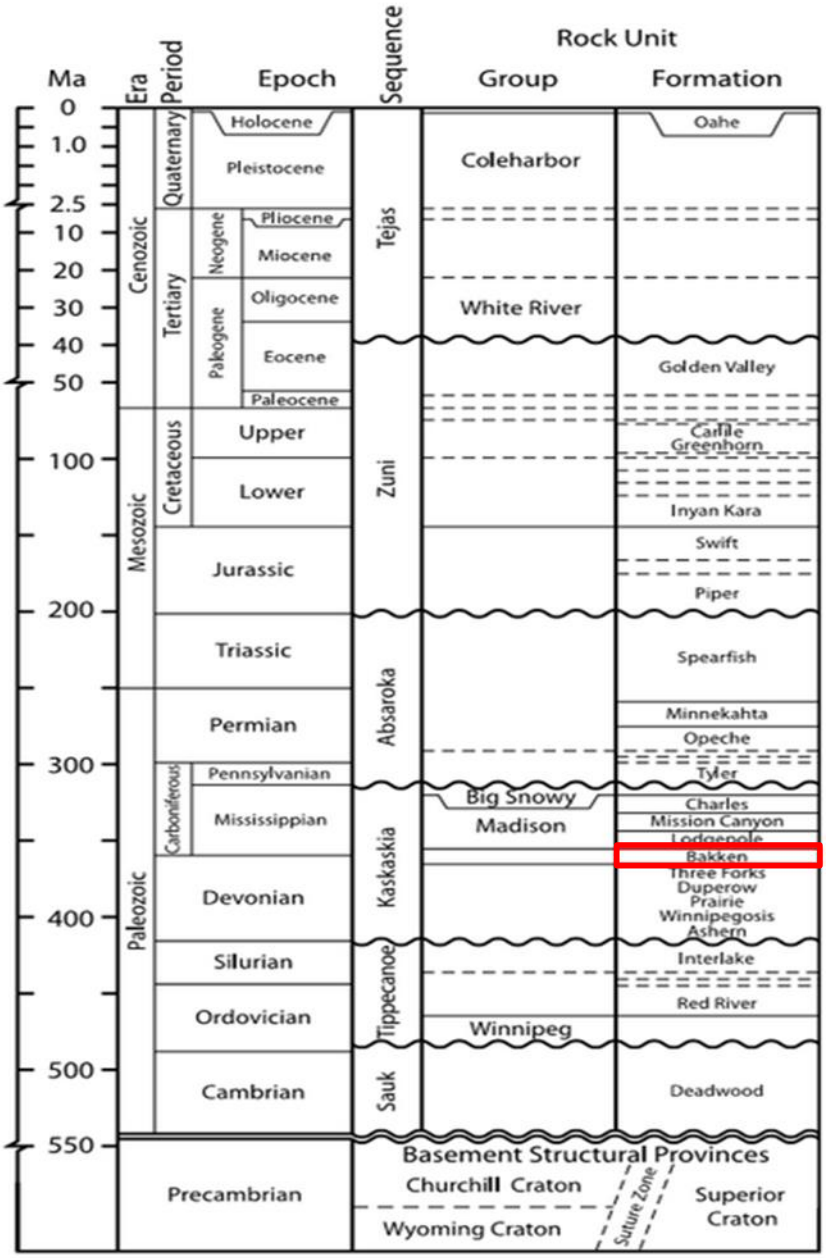

Figure 2-5 Generalized stratigraphic column for the Williston Basin with Bakken Formation shown in red (modified from Kuhn et al., 2012).

2.3 Stratigraphy of the Bakken Formation

The Bakken Formation is an Upper Devonian through Lower Mississippian unit of the Williston Basin. It overlies the Devonian Three-Forks Formation and is overlain by the Mississippian Lodgepole Formation (Figures 2.5, 2.6). It has a thickness of about 50 m (<160 ft), extends blanket-like in the subsurface of the Williston Basin at a maximum depth of 3700 m (~12,150 ft.) and can be correlated across the basin, from its distinct gamma-ray well-log pattern (LeFever, 2005, Kuhn et al., 2012).

Bakken Formation is divided into three member units: the Upper Bakken shale member, the middle reservoir member and the Lower Bakken shale member (Webster, 1984, LeFever, 2008). The upper and lower Bakken shales are black organic-rich marine shale. They are both of homogeneous lithology, act as the major source rocks feeding the middle member and have very high gamma ray readings (>200 API) and low resistivity readings. Olesen (2010) reported they also tend to exhibit some brittleness due to high silica content. The Middle Member varies in lithology, has a typical wireline log characteristics for clastics and carbonates and acts as the major reservoir in the Bakken petroleum system. Kuhn et al. (2012) and Sonnenberg (2014) both reported the production from the Upper Shale, while Sarg (2012) reported that reservoirs are present both in the Middle Bakken Member and Upper Bakken Shale. Price and LeFever (1994) reported that the Bakken oils were confined to the Bakken source system

(uppermost Three Forks Formation to lowermost Lodgepole Formation) and have not migrated into the overlying Mississippian reservoirs.

Depositional environments interpreted for the Bakken Formation have ranged from a marine swamp with a restricted circulation caused by the prolific growth of organic matter to an offshore marine environment with a stratified water column (LeFever, 1991). Each of the three Bakken members extends across a wider area than the preceding one, as they tend to pinch out against the Devonian Three Forks Formation (Figure 2.6).

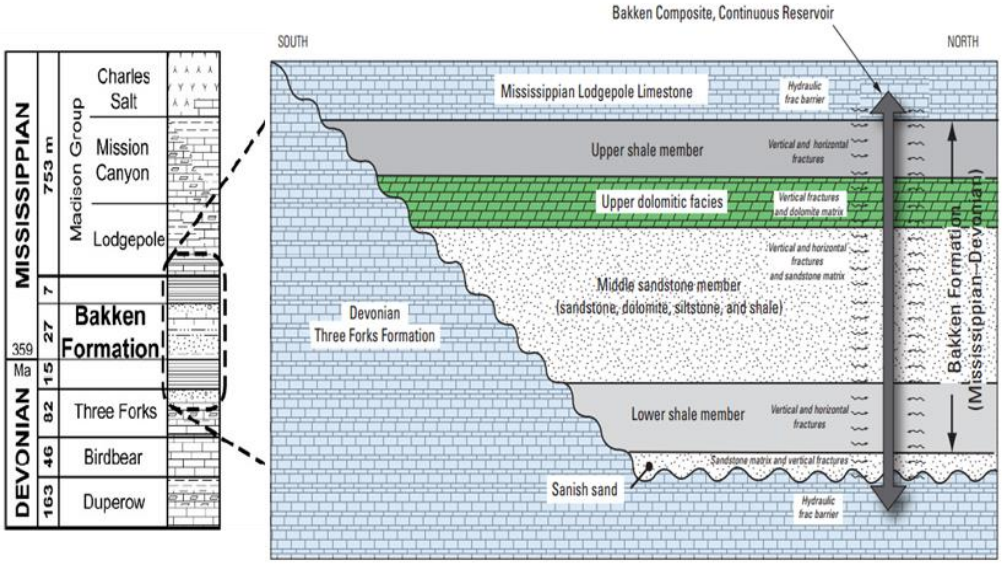

Figure 2-6 Schematic stratigraphic column of the Bakken Formation with overlying and underlying Lodgepole and Three-Forks Formations respectively [modified from Kuhn et al., (2012) and Pollastro et al., (2010)]

2.3.1 Upper Bakken Member

The lithology of the upper member of the Bakken Formation homogenously consists of dark grey to brownish-black to black, fissile, noncalcareous, bituminous and carbonaceous shale (Meissner 1978, LeFever 1991). It is slightly to highly rich in organic carbon (up to 35% TOC), with laminated-to-massive bedding of silt-sized material occurring throughout and a lag unit of conodonts, fish bones and teeth, with phosphatic grains commonly at the base (Pollastro et al., 2013). Fractures are also present in the upper shale member that reaches a maximum thickness of 28 ft. (9 m) in North Dakota (LeFever, 1991). It has been reported as being brittle due to its high silica content. The isopach maps of LeFever, (2008) show that the member has a broad, yet poorly defined, depocenter. The Upper Member of Bakken is characterized by high gamma-ray, very-high to very-low resistivity in a typical log (Figure 2.7), has a reported average porosity 5.5%, and a permeability of 0.1mD (Meissner, 1978).

2.3.2 Middle Bakken Member

The Bakken Middle Member in North Dakota has a variable lithology ranging from light grey to medium grey interbedded sequence of siltstones and sandstones with lesser amount of shale, dolostones and limestones rich in silt, sand and oolites present (LeFever, 1991; Pitman et al., 2001; Kuhn et al., 2012). The siltstones and sandstones are massively or coarsely bedded with occasional trough or planar cross-bedding. The middle member, sandwiched between the

upper and lower members, is the thickest of the Bakken Formation with a maximum thickness of 87 ft. (27 m) in North Dakota, and a well-developed depocenter (LeFever 1991; Pollastro et al., 2010).

Several studies have identified and mapped various lithofacies within the Middle Member of the Bakken Formation. Smith and Bustin (2000) and Sarg (2012) identified six lithofacies, while LeFever (2007) recognized seven lithofacies. Sarg (2012) described the depositional environment of the middle member to be from shallow water marine environment. The Middle Member is also the major reservoir member and the main focus of exploration within the Bakken petroleum system.

2.3.3 Lower Bakken Member

The Lower Shale Member of the Bakken Formation is similar to the Upper Member. It consist of dark-grey to brownish-black to black, quartz-rich, massive to fissile, non-calcareous, slightly to highly organic-rich shale (LeFever et al.,1991; Pitman et al., 2001; Pollastro et al., 2010; Kuhn et al., 2012). It has the smallest geographic extent with a well-defined depocenter and reaches a maximum thickness of 56 ft. (17 m) (Pollastro et al., 2010). The lithology is similar to the upper shale member, however, the color of the shale varies depending on the amount of silt versus clay and carbon present. Thin laminae of siltstone, limestone and sandstone and lag deposits containing fragments of conodonts, fish bones and teeth, with phosphatic particles are locally present at

the base of the member (LeFever et al., 1991). The Lower Shale is also considered to be a mature source rock with occasional fractures present.

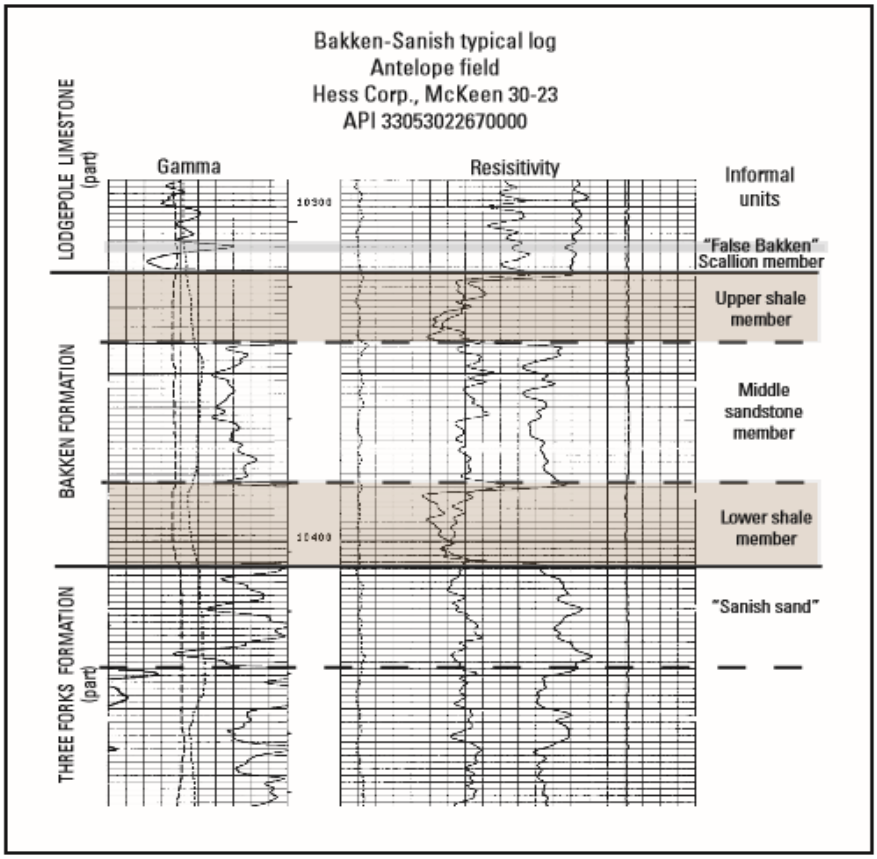

Figure 2-7 Typical gamma-ray and resistivity curves of the three members of the Bakken Formation from Antelope oilfield, McKenzie County, N. Dakota (from Pollastro et al., 2010)

Chapter 3

Methods of Study

3.1 Sampling Procedure

This study focuses on three core samples collected from a well in a producing field of the Williston Basin in North Dakota. These cores which were continuous with very few missing intervals were obtained from the core library and laboratory of the North Dakota Geologic Survey. About two inches were cut from each member of the Bakken Formation with the help of the Laboratory Technician based on intervals in the well reports, well-logs and visual identification. Figures 3.1 and 3.2 show the images of the Bakken cores of the well from the core library and after they were sampled at chosen intervals.

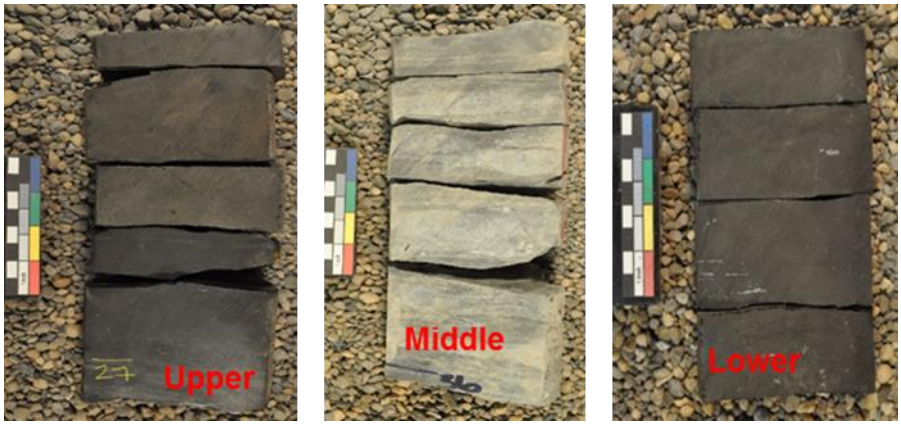

Figure 3-1 Photos of Kubas well cores of each Bakken members taken from core box before they were cut from North Dakota Geological Survey

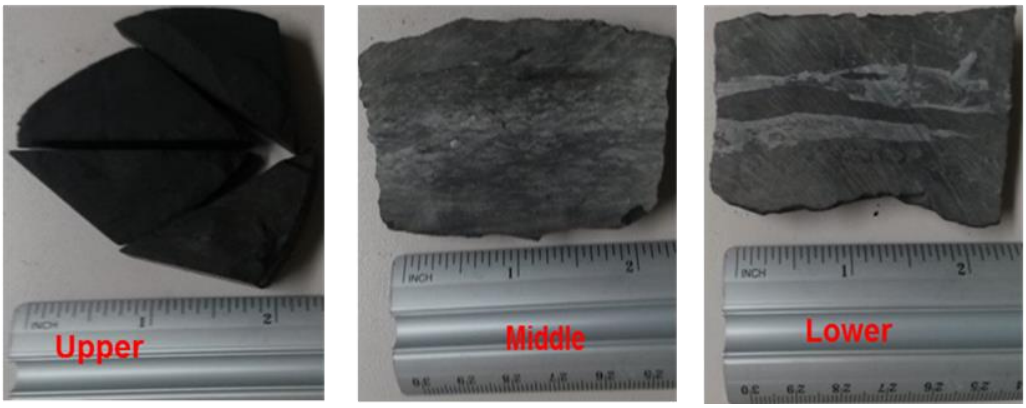

Figure 3-2 Photos of freshly-cut Kubas well cores of each Bakken members from well obtained from North Dakota Geological Survey.

3.2 Mercury Injection Capillary Pressure (MICP)

Mercury Injection Capillary Pressure was used to measure the pore throat distribution in a sample and also measures the connected pore space based on the capillary pressure measurement within the sample. This experiment was conducted on 2-3 grams of sample fragments and it involves the use of non-wetting mercury to invade pore throats by overcoming the capillary pressure through applied external pressure of 60,000psia (413MPa). The apparatus used is the Micromeritrics Autopore IV 9510 (Norcross GA) capable of producing such high pressure and this corresponds with the Washburn Equation for a pore diameter of 3 nanometers (nm) to 300 µm. (Figure 3.3).

As a non-wetting fluid for most porous media, mercury will not invade pores unless an external pressure is applied. The diameter of the pores invaded by mercury is inversely proportional to the applied pressure, as higher pressure is required to force mercury into smaller pores. Washburn (1921) developed the

following equation based on the assumption that all the pores are cylindrical in shape:

The experiment is based on Washburn's equation stated as;

$$\Delta P = \frac{-2W\alpha Cos\theta}{R} \quad \text{...(3.1)}$$

Where,

R = equivalent pore-throat radius (µm), W = Washburn unit conversion factor (0.145)

α = surface tension of mercury (485 dynes/cm for Hg), θ = contact angle between mercury and the porous medium(130° for Hg in most solids), ΔP = pressure difference across the curved mercury interface (psia).

$$\Delta P = {}^{90.4}/_{R} \quad \text{.. (3.2)}$$

Each sample was oven-dried at 60 °C for at least 48 hours to remove moisture, then cooled to room temperature (~23 °C) in a desiccator before the MICP test. Samples were then evacuated to 50 µm Hg (0.05 Torr or 6.7 Pa). During the MICP test, each sample underwent both low-pressure and high-pressure analyses. Under low-pressure analysis, the largest pore-throat diameter recorded by MICP is about 300 µm. Equilibration time (the minimum time duration to achieve a stable mercury level before proceeding to the next pressure) was chosen to be 50 seconds. Since pore throats control access to the pore space, mercury first fills up the pore space it can access through the largest

pore throats by overcoming capillary pressure, it then passes through smaller and smaller pore throats as pressure increases and eventually fills up the entire connected pore space. At 60,000 psi pressure, mercury can enter pore throats as small as 3 nm in diameter. The intrusion volume is recorded and after reaching the 60,000 psi, the pressure is reduced to allow for extrusion and the extrusion volume is recorded.

Because the interfacial tension of mercury and contact angle between mercury and rock sample is already known, knowing the pressure at which the mercury passes through the pore throats and the pore throat radius can be estimated along with porosity, permeability and tortuosity.

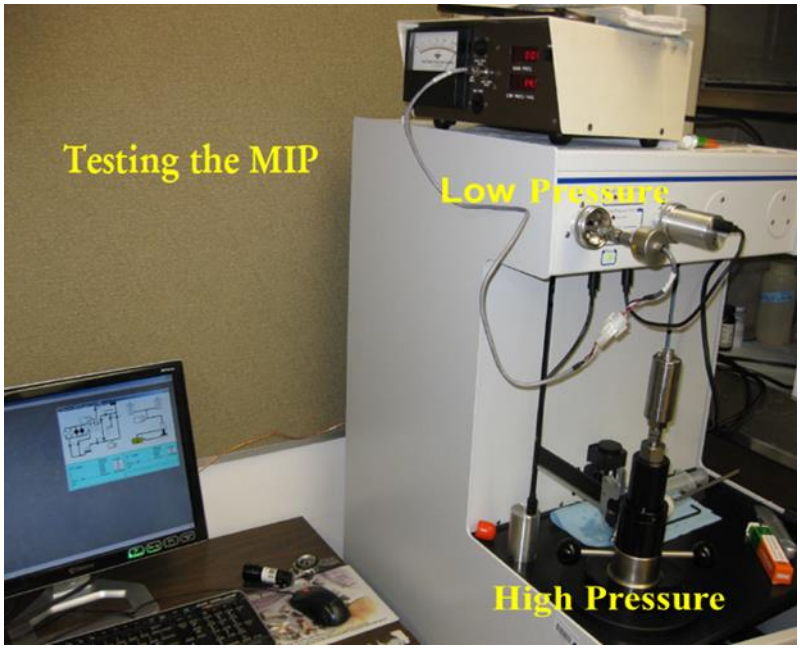

Figure 3-3 AutoPore IV® machine used to run Hg injection porosimetry experiments

During the sample analysis, MICP tend to collect the data from the applied pressure and cumulative intrusion volume at that specific pressure. As reported by Gao and Hu (2013), porosity, median pore-throat diameter, and permeability for the shale samples were calculated by the method of Katz and Thompson (1986; 1987) from the following equation:

$$k = 1/89(L_{max})^2 (L_{max}/L_c)\, \phi\, S(L_{max}) \quad \text{(3.3)}$$

where $\boldsymbol{k}$ (darcy) is the permeability; $\boldsymbol{L_{max}}$ (μm) is the pore-throat diameter at which hydraulic conductance is maximum; $\boldsymbol{L_c}$ (μm) is the characteristic length which is the pore-throat diameter corresponding to the threshold pressure Pt (psia); $\boldsymbol{\phi}$ is the porosity; $\boldsymbol{S(L_{max})}$ represents the fraction of connected pore space composed of pore width of size L_{max} and larger.

After the experiment, the data obtained during the intrusion and extrusion cycles are further used to plot incremental and cumulative mercury intrusion curves. The incremental intrusion or pore volume curve is obtained from plotting incremental mercury intrusion against pore throat diameter as a function of pressure. The cumulative intrusion for a pressure point is calculated by summing up the incremental intrusion at all pressure points less than and equal to that of the pressure point. A cumulative mercury intrusion curve is obtained when these data are plotted against pressure or pore-throat diameters. Incremental intrusion curves are typically made by including data obtained during intrusion cycle only. Cumulative intrusion curves are made by including the data points from intrusion as well as from extrusion cycle. It should be noted that not all the mercury that enters the pores comes out during extrusion cycle and as such hysteresis is

observed in the plot. The presence of the hysteresis confirms that the intrusion was real and the experiment was correctly done.

3.3 Fluid Imbibition Tests

Spontaneous imbibition is a process driven by capillary-force whereby a wetting fluid displaces a non-wetting fluid under the influence of capillary suction only. During the process of secondary oil recovery from fractured reservoirs, fluid is spontaneously imbibed from the fracture system into the rock matrix blocks, thereby resulting to the oil and gas in the matrix being displaced by the fluid. Going by this, it's fine to say that the oil/gas secondary production rate is strongly dependent on the spontaneous imbibition process, and extensive research has been undertaken to investigate this process in oil and gas industry (Li, 2007; Olafuyi et al., 2007; Standnes, 2010; Shahri et al., 2012; Wang 2012).

The imbibition test involves exposing one face of a rock sample to fluid, and measuring the mass of fluid uptake over time. This test is a simple procedure for probing pore connectivity within a sample matrix, and for estimating the crossover length (depth to constant accessible porosity) in low pore connectivity rocks (Hu et al., 2001; 2012). Based on the network modeling results of Ewing and Horton (2002), we can probe pore connectivity, as indicated by the slope from the log plot of imbibed liquid mass versus log time. The imbibition behavior slope of ¼, ¼ changing to ½, or ½ – roughly classifies a rock's pore connectivity (Hu et al., 2012).

Imbibition is mathematically analogous to diffusion in that, for classical homogeneous materials under negligible gravitational effects, the distance *l,* to the wetting front increases with the square root of time ($l \sim t^{0.5}$), (Hu et al., 2012). If the accessible porosity is uniform with distance, then the cumulative mass of imbibed water *I* behaves identically as $I \sim t^{0.5}$. The mass is plotted against the square root of time after the experiments. The slope obtained is usually around 0.5 for well-connected pores and 0.25 or less for poorly connected pores (Ewing and Horton, 2002). If the accessible porosity is uniform with distance, then the cumulative mass of imbibed water *I* behaves identically: $I \sim t^{0.5}$. This relationship gives a slope of 0.5 in log space, which we call the imbibition slope.

Core samples of approximately 1cm cube were cut from the blocks of the Bakken samples from a producing well (Kubas) and labelled uniquely. The sample cubes were coated with quick-cure epoxy sealant leaving just two faces that will go into the fluid. This will ensure one dimensional imbibition to avoid evaporation of the imbibing fluid from (and avoid vapor transport and capillary condensation through it) the side surfaces of the samples (Figures 3.4 A, B and C). Once the epoxied samples were dried, they were placed in a 60°oven to dry up residual fluid. The dried sample is then placed in a desiccator to cool off for about 2 hours and then taken out for the experiment. A dish is filled with fluid (DI water without tracers, API brine or n-decane with tracers) and the weight was recorded. The sample dimensions and weight were also recorded.

Figure 3-4 Labelled sample cubes coated with quick cure epoxy; prior to imbibition

The experiment were performed by bringing the non-epoxied face of the sample into contact with the dish solution and recording the weight change over time automatically into a computer connected with the apparatus (Figure 3.5). The core was suspended from a hook underneath the electronic balance and in a closed chamber while the major part of the sample remains suspended in the air leaving just the exposed face to make contact with the fluid.

For water imbibition experiments, beakers of water were placed inside the experiment chamber to keep the humidity inside the chamber constant. The top side of the epoxied samples were loosely covered with foil, with a small hole left for air escape, to reduce vapor transport and capillary condensation on to the top face. The sample bottom was submerged to a depth of about 1 mm in a fluid reservoir. The imbibition rate was monitored by automatically recording the sample weight change over time. The imbibition experiment was done in a

direction that is parallel to the bedding plane on the sample. The maximum relative error of the measurements is estimated as ±20 seconds. The tracer solution containing both nonsorbing (bromide and perrhenate) and sorbing (cesium, cobalt, samarium, and strontium) tracers was prepared using ultrapure (Type 1) water and >99% pure reagents ($CoBr_2$, CsBr, CsI, NaBr, $NaReO_4$, $SmBr_3 \cdot 6H_2O$, $SrBr_2 \cdot 2H_2O$). The tracers in the n-decane include organic-iodine (iododecane) and trichlorooxobis (triphenylphosphine) rhenium (V). After the tracer experiment, the samples were frozen with liquid nitrogen, freeze-dried at -52 °C and near-vacuum (about 1 Pa) for a day, and then stored at relative humidity below 10% before elemental mapping.

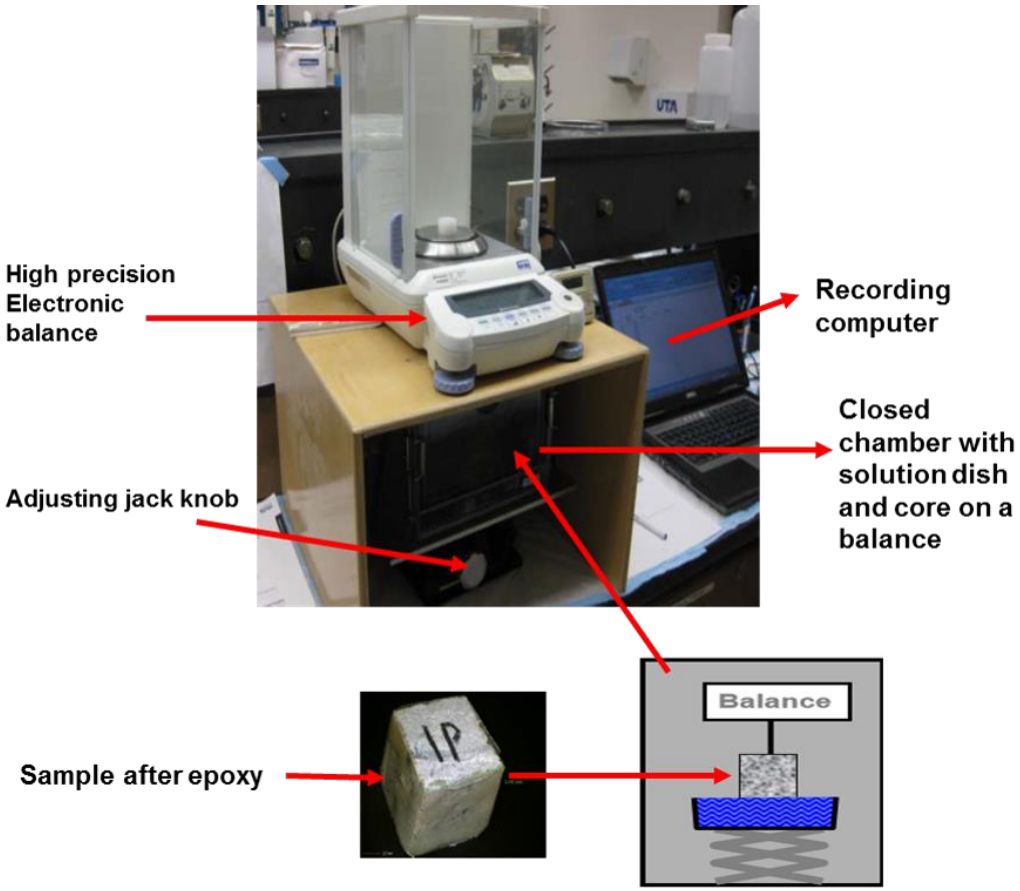

Figure 3-5 Apparatus for spontaneous imbibition experiments, consisting of electronic balance, hook to hold the sample and computer to record readings

3.4 Saturated Diffusion Tests

The purpose of this experiment is to measure the pattern of solute diffusion in cm-sized samples and the decrease in accessible porosity with distance from an exposed face. This is done in order to assess the pore connectivity in the Bakken samples. In this experiment, dry shale samples were placed in a chamber which was then evacuated for 18 to 24 hours at 99.99% vacuum to remove all of the absorbed water and volatiles from the edge

connected pores. Then a saturating fluid made up of n-decane (no tracers) is introduced into the system so as to allow the fluid to penetrate and occupy the evacuated pores of the sample. Following the approach published in Hu and Mao (2012), the samples were then placed on a Teflon mesh inside a traced-decane solution reservoir, such that only the bottom of the sample (to reduce hydraulic head differences) touched the tracer solution, which was constantly stirred with a magnetic stirrer. The reservoir volume was on the order of 320 mL, compared to the samples' pore volume of less than 0.1 mL. This high volume ratio ensured an approximately constant tracer concentration (as required to satisfy the boundary condition of the applicable mathematical solution of the diffusion equation).

Figure 3-6 Apparatus for the saturated diffusion experiment; consist of stop clock and lidded reservoir holding the tracers solution during an experiment

The lidded reservoir was held at a constant 23 °C. After a fixed diffusion time of 25 hours, the samples were removed from the reservoir, frozen with liquid nitrogen, freeze-dried at -52 °C and near-vacuum (about 1 Pa) for a day, then stored at relative humidity below 10% prior to LA–ICP–MS (laser ablation-inductively coupled plasma-mass spectrometry) analyses.

3.5 Tracer Mapping by Laser Ablation-Inductively Coupled Plasma-Mass Spectrometry (LA–ICP–MS)

In this Task, we measure the decrease in accessible porosity with distance from an exposed face in order to assess pore connectivity in the shale samples. This is because in a rock with sparsely-connected pores, the accessible porosity decreases with distance from an edge (a fracture for example).

For this test, tracers in fluids are used to specifically interrogate the wettability of kerogen and mineral pore spaces and their connectivity, by conducting diffusion and imbibition tests. Two molecular tracers and their sizes used in *n*-decane are the organic iodine (1-iododecane) with dimension of 1.393 nm×0.287 nm×0.178 nm for and the trichlorooxobis (triphenylphosphine) rhenium (V) with dimensions of 1.273 nm×0.919 nm×0.785 nm. The tracers were chosen because they are non-sorbing, easily detectable by LA-ICP-MS analysis and will only occupy accessible pores without reacting with the matrix.

After tracer imbibition and diffusion tests, whether with brine or n-decane, the Bakken samples were frozen with liquid nitrogen, kept at -80°C in a freezer, freeze-dried, then stored at <10% relative humidity until LA–ICP–MS analysis.

The tracer distribution in the samples is then mapped with laser ablation-inductively coupled plasma-mass spectrometry. Prior to cutting, both the top (tracer-exit) and bottom (tracer-entry) faces were spot-checked for the presence of tracers, and then the sample was cut dry in the middle from the top face. This was done transverse-wise with respect to the imbibition or diffusion direction, using a low-speed diamond saw (Buehler IsoMet). The laser ablation system (New Wave; Freemont, CA) (Figure 3.6) used a 100 μm spot diameter UP-213 laser to vaporize a hole in the shale sample at sub-micron depth increments; elements entrained in the vapor were analyzed with ICP–MS (PerkinElmer/SCIEX ELAN DRC II; Sheldon, CT). This LA–ICP–MS approach can generate 2-D and 3-D maps of chemical distributions in rock at a spatial resolution of microns, and a concentration limit of low-mg/kg (Hu et al., 2012; Peng et al., 2012; Hu and Mao, 2013).

Figure 3-7 The LA–ICP–MS apparatus for micro-scale elemental mapping of tracer distribution patterns in the samples

Chapter 4

Observations and Results

4.1 Mercury-Injection Capillary Pressure (MICP)

Mercury intrusion measurements were carried out to obtain the pore-throat distributions of the three Bakken members at their respective depths from Kubas Well in Stark County. The results showing pore-throats distribution were plotted on a scatter chart of measured pore volumes versus pore-throat diameters (Figures 4.1, 4.2 and 4.3) and on a histogram (Figure 4.4) The MICP results show that most pores (about 70–80% by volume) in the Bakken samples are smaller than 1 μm. As measured by the MICP, pores in the three members of Bakken Formation are predominantly in nanometer size range while the estimated permeability are in nanodarcy.

The MICP results shows the Bakken members have average pore-throat diameters of 7.8 nm, 6.8 nm and 17.6 nm, with estimated permeability of 3.16, 0.85, 5.68 nanodarcies for the Upper, Middle and Lower Bakken respectively. The pore throat distributions for the three members were also plotted. These values are slightly deviated from the published values but still falls within the range of what is expected from a poorly connected rock. Aside from the pore-throat diameters, permeability estimates were obtained from the analyses, as well as other useful petrophysical parameters such as porosity and tortuosity (Table 4-1).

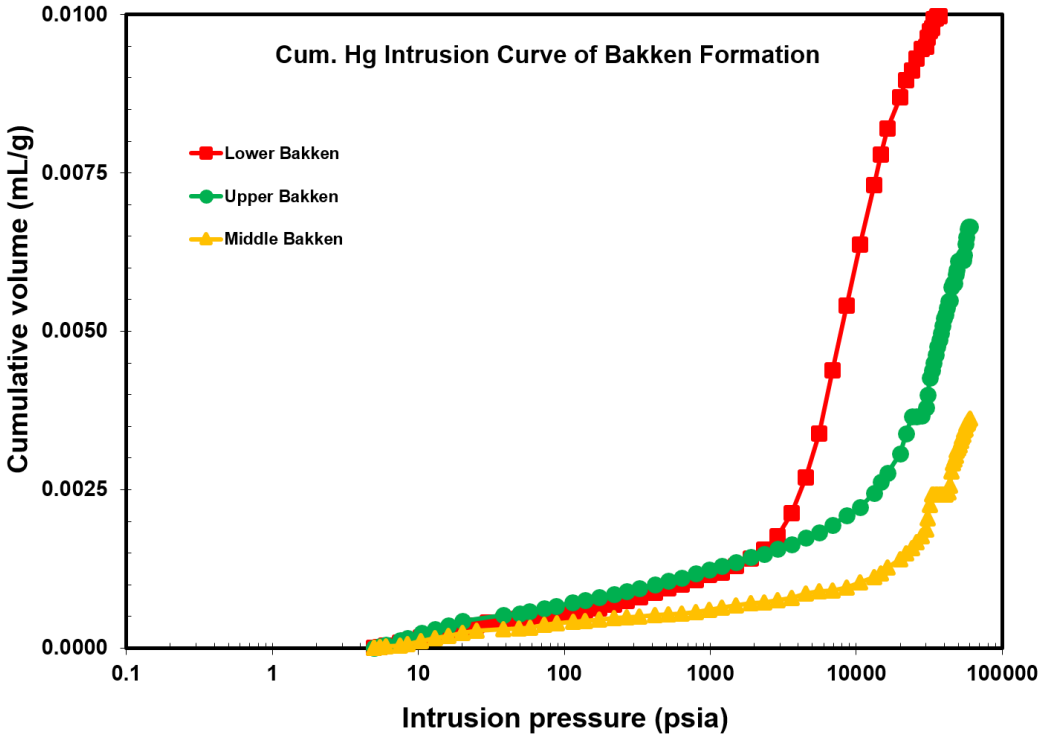

Figure 4-1 MICP analysis of Bakken Formation showing cumulative mercury intrusion volume versus intrusion pressure for the three Bakken Members.

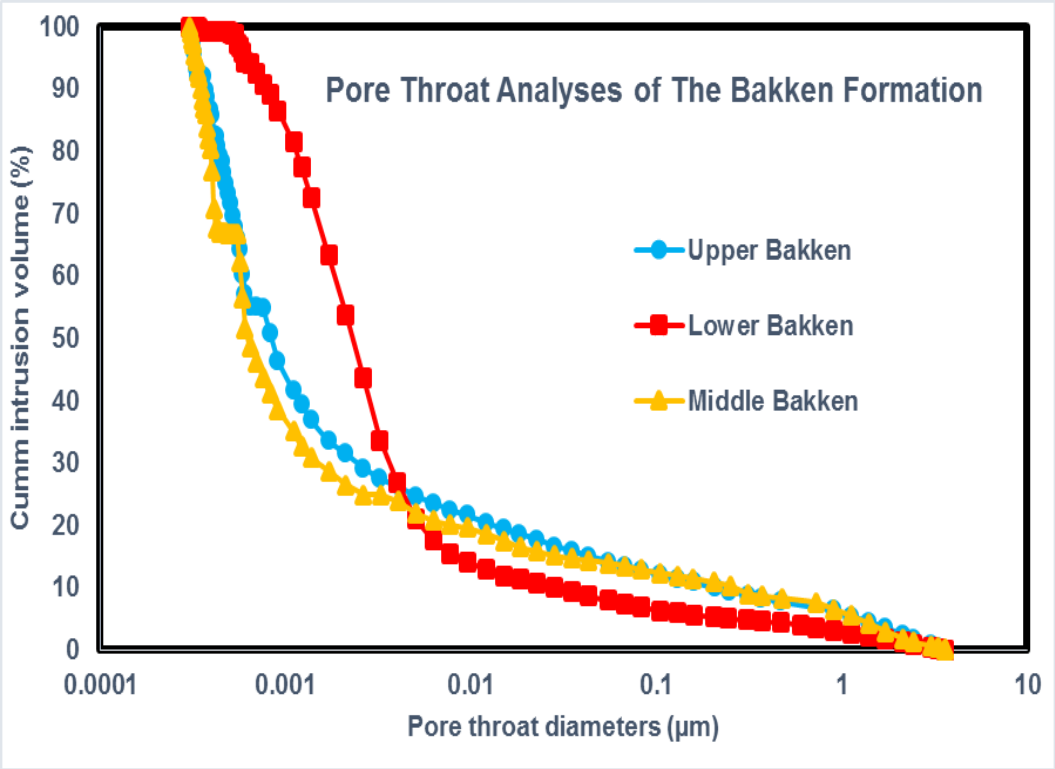

Figure 4-2 Comparison of pore-throat diameters of the three Bakken Members from MICP analyses showing distribution cumulative intrusion volume versus pore-throat diameter

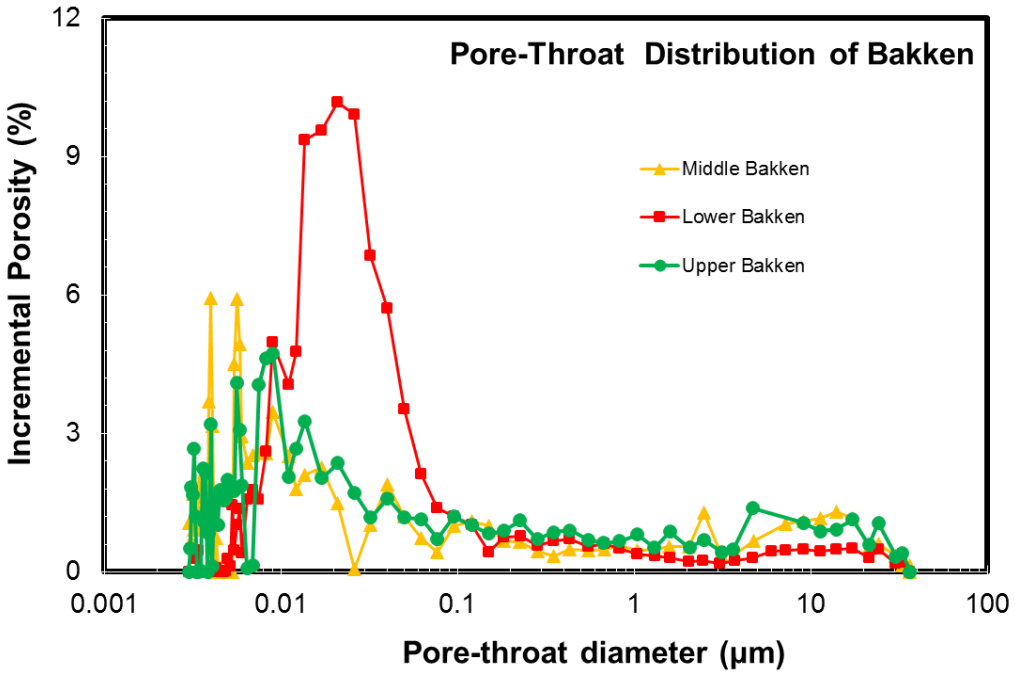

Figure 4-3 Comparison of pore-throat diameters of three Bakken Members from MICP analyses showing distribution cumulative intrusion volume versus pore-throat diameter

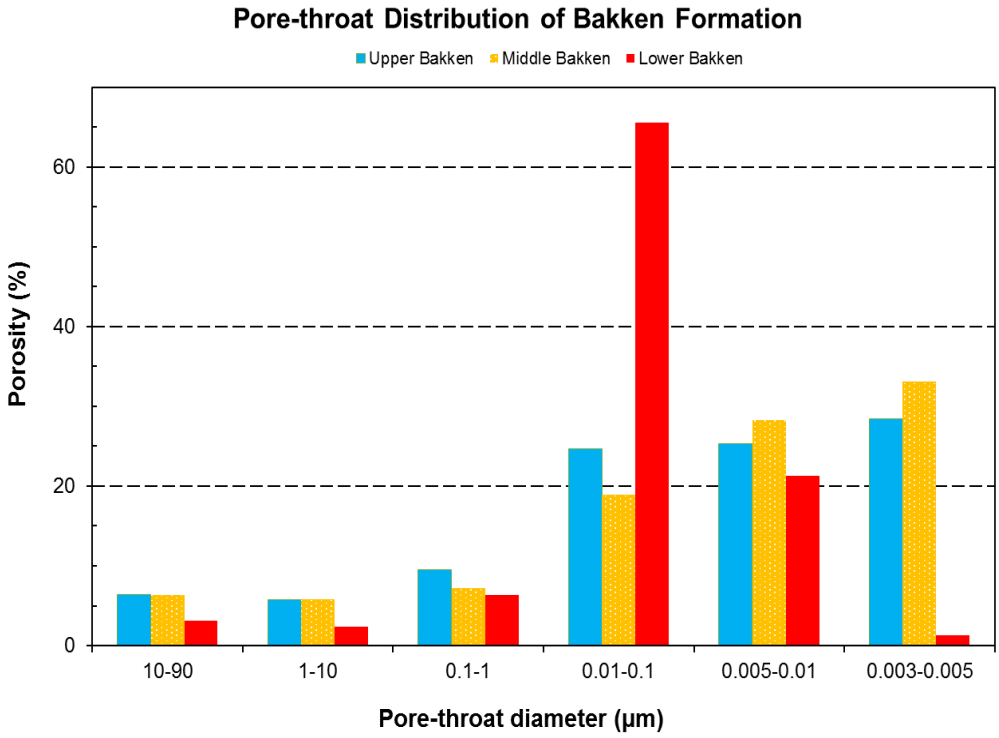

Figure 4-4 MICP analysis of Bakken Formation on a histogram showing porosity versus pore-throat diameter for three Bakken members

Table 4-1 Result summary of the MIP experiment; Le is the effective path length through the pores, while L is the length of the core sample

Sample	Sample Depths (ft)	Median Pore-throat Diameter (nm)	Average Pore-throat Diameter (nm)	Porosity (%)	Permeability (nanodarcy)	Le/L [square root of (tortuosity*ϕ)]
Kubas Upper Bakken	10626	8.4	7.8	1.62	1.82	6.4
Kubas Middle Bakken	10636	6.2	6.8	0.98	0.85	5.23
Kubas Lower Bakken	10638	22.8	17.6	2.76	37.2	3.89

During the experiment, mercury starts to intrude from the larger pores to the tiny pore sizes as the pressure increases. Thus higher pressure is needed to invade tighter pore throats. The incremental intrusion curve represents the pore volume accessed through pore-throats of a given grain size. The intrusion saturation starts at zero and then increases as pressure reaches 60,000 psia and volume of mercury forced into the rock at 100% is the limit of the machine. The 100% mark was set at the limit of the machine, but from figure (4.2), we observed continuity beyond the mark. This implies that there are still pores below the 3nm limit of the machine. This pores (< 3nm) can be studied using nitrogen sorption test. The result shows that the Lower Shale Member have the highest porosity

and pore-throat diameters. However both shale members have higher porosity and pore-throat diameters than the Middle Member, and this may be attributed to more (larger) natural fractures. Samples with higher pore diameters are often expected to have higher permeability as observed in the Lower Members of the Bakken Formation (Table 4-1).

The tortuosity observed were also fairly large and the effect were observed fluid imbibition within the Bakken members. For tight matrix, mercury requires as much 60,000 psia to achieve significant intrusion, hence, for this tight rocks, the higher the pressure at which the mercury intrusion occurs, the lower the permeability.

4.2 Fluid and Tracer Imbibition

Imbibition tests from the three Bakken members produced slopes ranging from 0.18 to 0.36 (Figures 4.4 to 4.6) indicating the low connectivity of the Bakken petroleum system. The result is based on the pore volume of fluid imbibed against time and the data is plotted for different fluid used for all three members of the Bakken Formation.

The slopes obtained are dependent on good pore networks, connectivity and wettability within the cores. The higher slope of 0.44 from the Upper Bakken using DI water as imbibition fluid (Table 4-2) does not mean good connectivity, it is rather the result of instability of the initial sample settling. Replicated test (using another sample) not reported produced a slope of 0.128. The imbibition test revealed fair connectivity with n-decane (0.363 through 0.386) and this is a

function of the Bakken wettability with oil. Low slopes were obtained from the brine and water imbibition tests and these slopes are indicative of the preferred oil-wet condition of the Bakken cores.

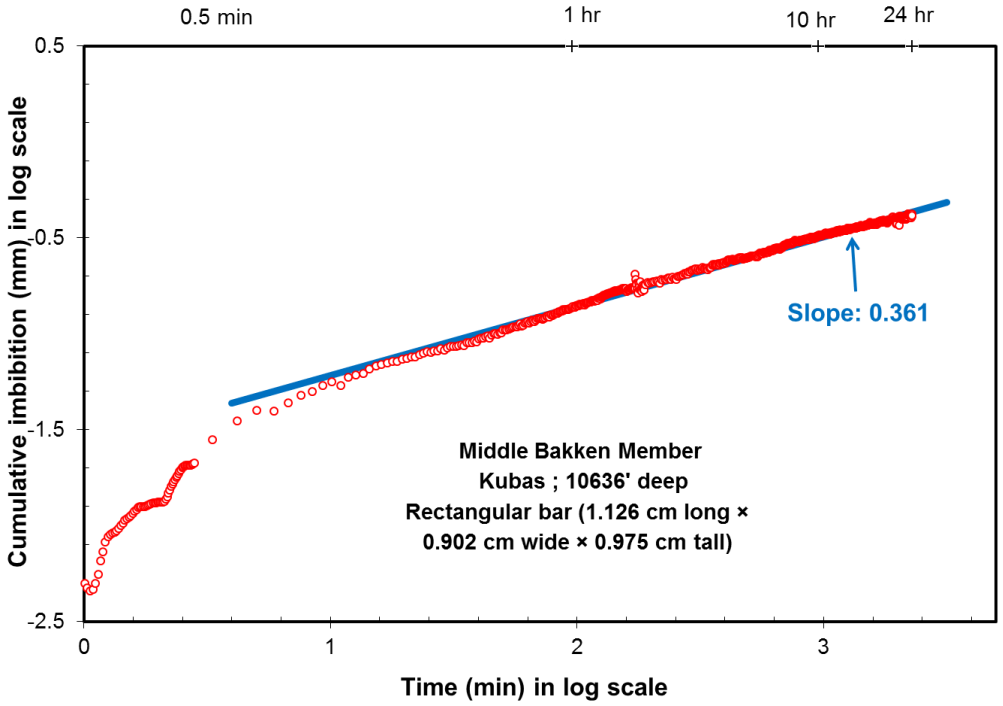

Figure 4-5 Imbibition curve and slope for the Middle Bakken: using n-decane with tracers as imbibition fluid

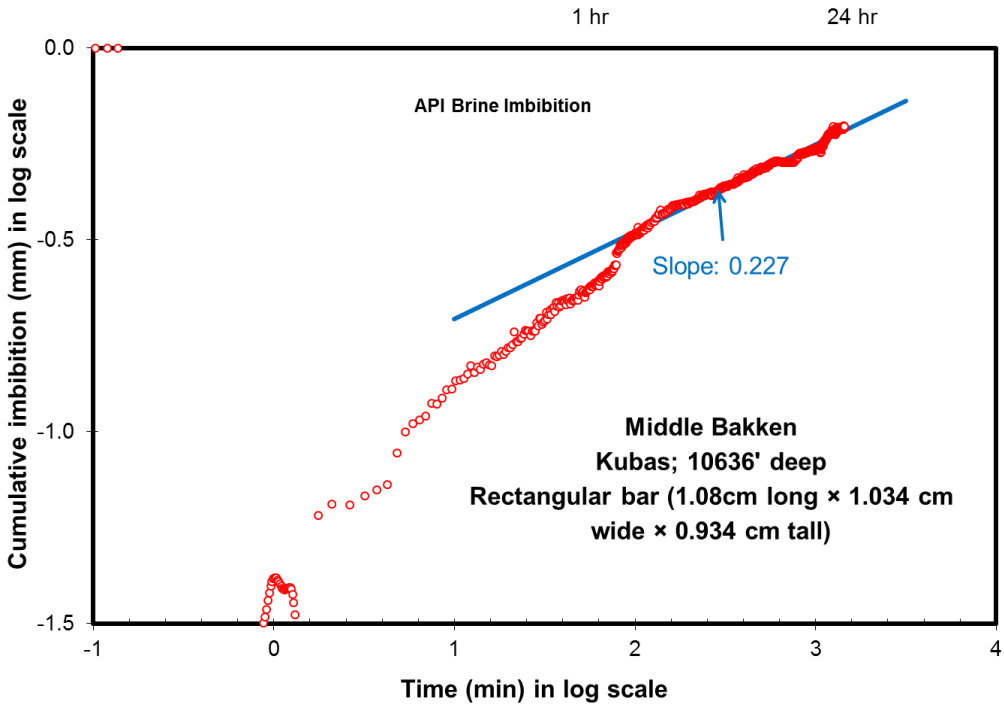

Figure 4-6 Imbibition curve and slope for the Middle Bakken: using API brine with tracers as imbibition fluid

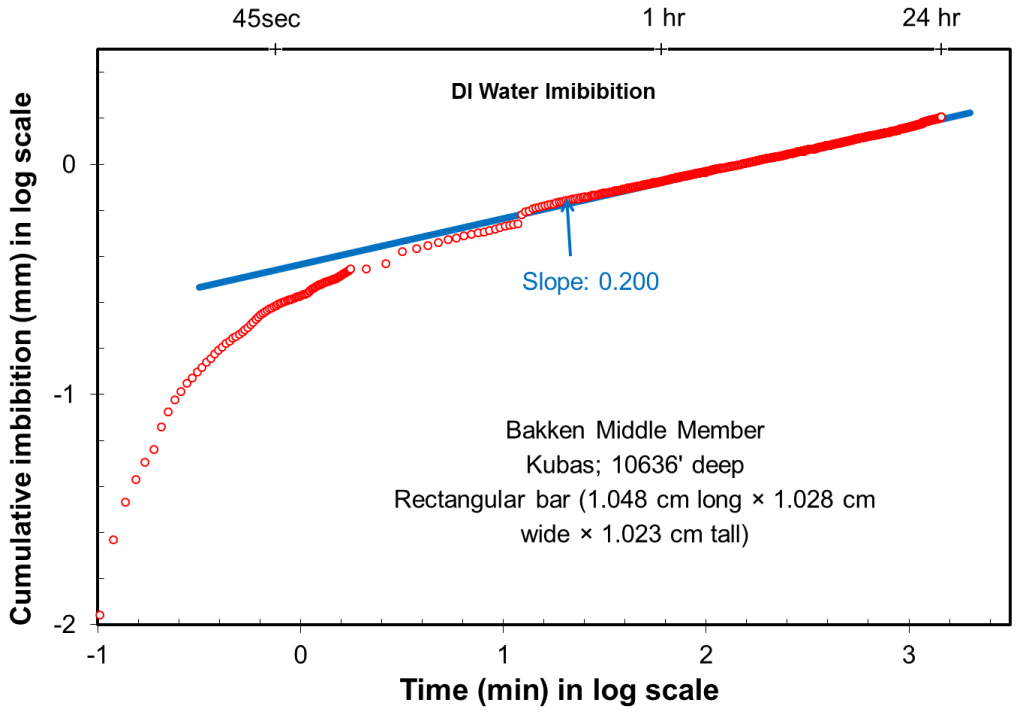

Figure 4-7 Imbibition curve and slope for the Middle Bakken: using DI water as imbibition fluid

Table 4-2 Behavior of imbibition slopes as a function of imbibing fluids

Rock Sample	Fluid	Sample Dimension (cm)	Time (Hr)	Imbibition Slope
Upper Bakken	n-decane with tracers	1.171 L × 1.163 W × 0.741 H	24	0.366
	DI Water	1.152 L × 1.075 W × 0.807 H	24	0.441
Middle Bakken	n-decane with tracers	1.126 L × 0.902 W × 0.975 H	24	0.363
	Brine with tracers	1.08 L × 1.034 W × 0.934 H	24	0.227
	DI Water	1.048 L × 1.028 W × 1.023 H	24 and 48	0.200; 0.250; 0.208
Lower Bakken	n-decane with tracers	1.095 L × 1.044 W × 1.040 H	24	0.386
	Brine with tracers	1.017 L × 9.83 W × 1.102 H	24	0.224
	DI Water	1.095 L × 1.044 W × 1.040 H	24	0.184

Based on the slopes alone, we cannot speculate or make a fair inference on poor connectivity of the Bakken pores for all fluids used (both water-and oil-wetting), however one important factor observed is in the wettability of the rocks. The imbibition curves favor the particular fluids used. A more pronounced curve and slopes were observed for n-decane fluid better than brine, from which we can infer about better fluid connectivity due to the wettability (oil-wet) of the samples.

4.2.1 Tracer imbibition and LA-ICP-MS Analyses

The tracer imbibition was also subjected through the LA-ICP-MS to map out the tracers distribution and the results yielded different tracer distribution

patterns (Figures 4.7 - 4.9). The non-colored portion on the map implies no tracer penetration in the pores as a result very tight pore throats. The pattern of pore penetration is a function of the molecular sizes of the tracers, made evident where organic-iodine which is smaller compared to the rhenium (V) penetrates more with higher concentration distribution in the sample.

The pattern, distribution and mass concentration of the tracers may also represent the patterns of the pores connectivity with respect to percolation theory. This can be observed from imbibition of the perrhenate (ReO_4^-) and europium (Eu^{3+}) ions as tracers in the brine fluid. The non-sorbing perrhenate tracer (ReO_4^-), is used as an indicative of the edge-accessible porosity distribution within the samples. As a non-sorbing tracer, ReO_4^- will only occupy the pore spaces equal or bigger than its molecular size without interacting with the shale matrix. Thus, the larger the pore spaces, the more concentration observed and, the better the connectivity pattern, the more pronounced the distribution pattern of the tracers within the sample. The dramatic decrease of tracers with depth illustrates the poorly-connected pore spaces of Bakken samples.

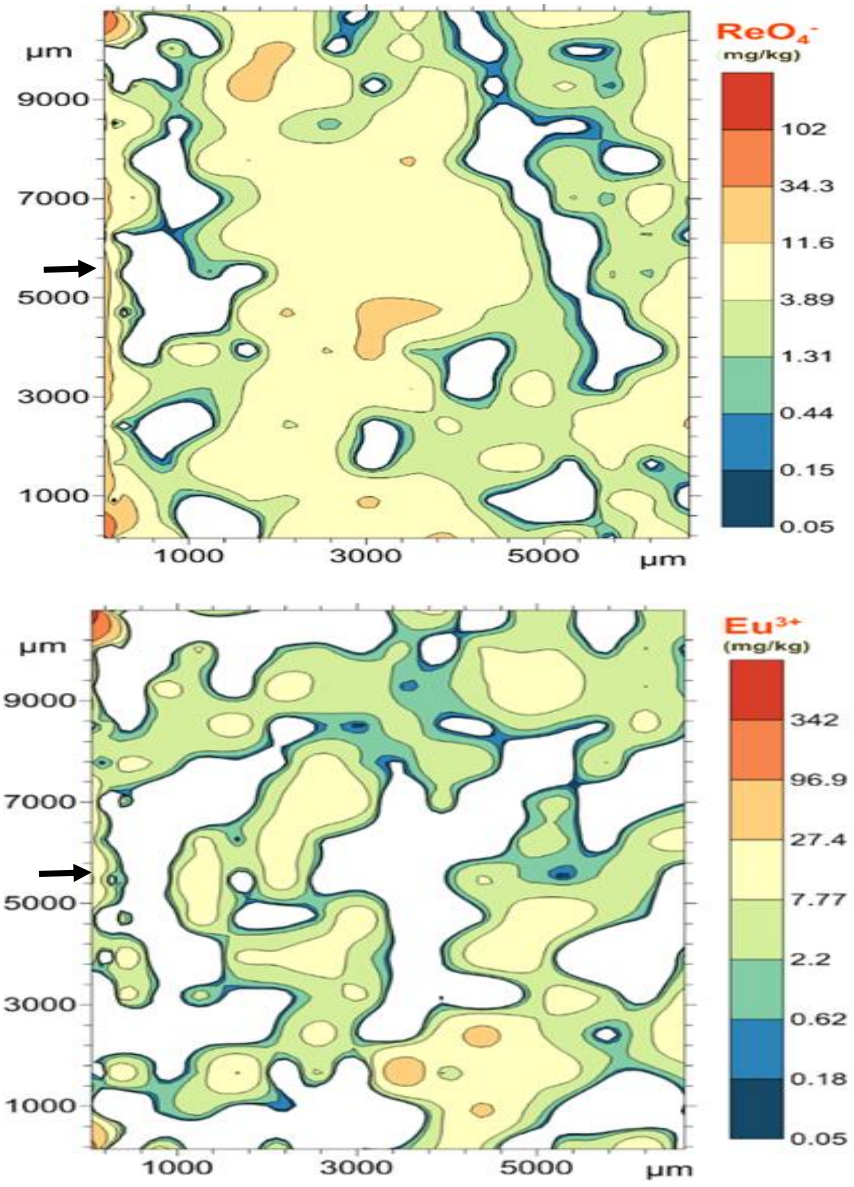

Figure 4-8 Traced-brine imbibition of ND Upper Bakken Member (interior face) using perrhenate and europium ions as tracers; arrows on the left indicate base of sample and direction of tracers' imbibition

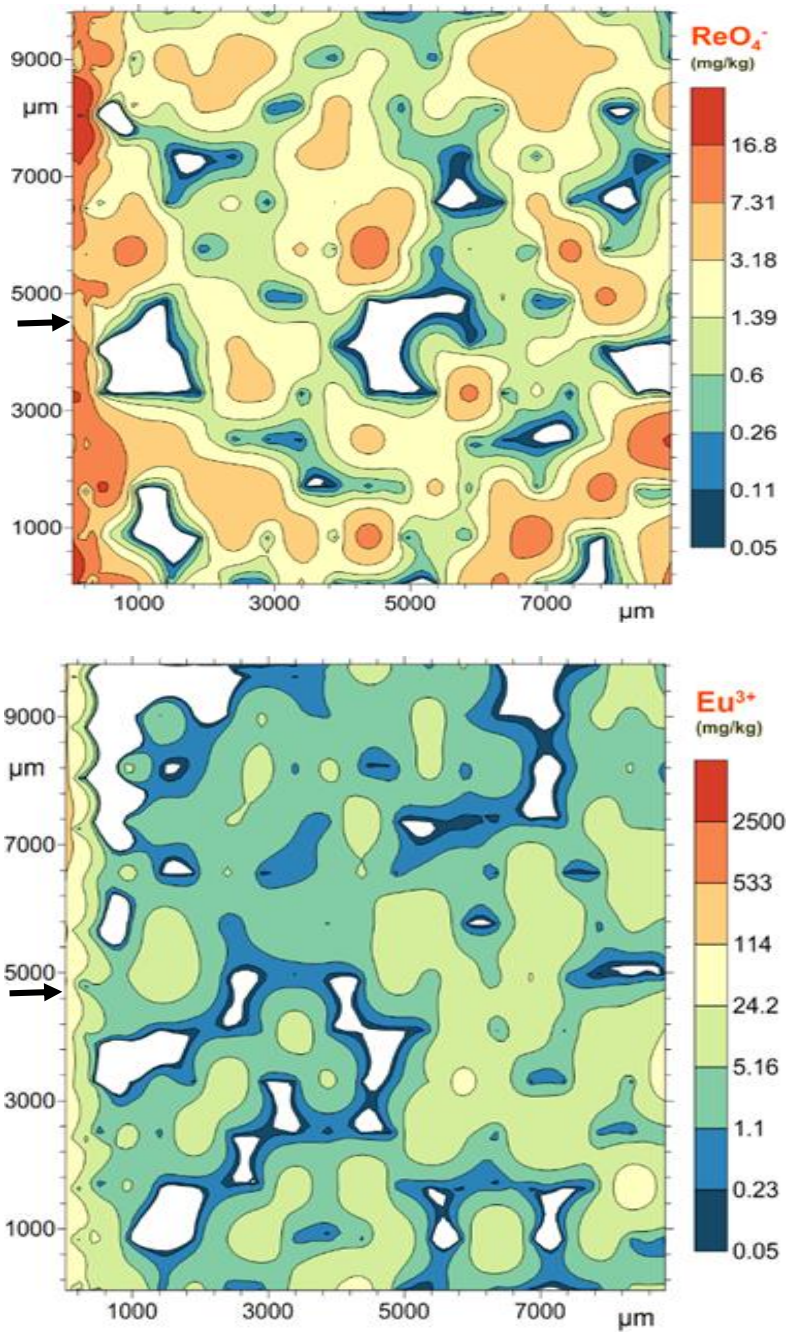

Figure 4-9 Traced-brine imbibition of ND Middle Bakken Member (interior face) using perrhenate and europium ions as tracers; arrows on the left indicate base of sample and direction of tracers' imbibition

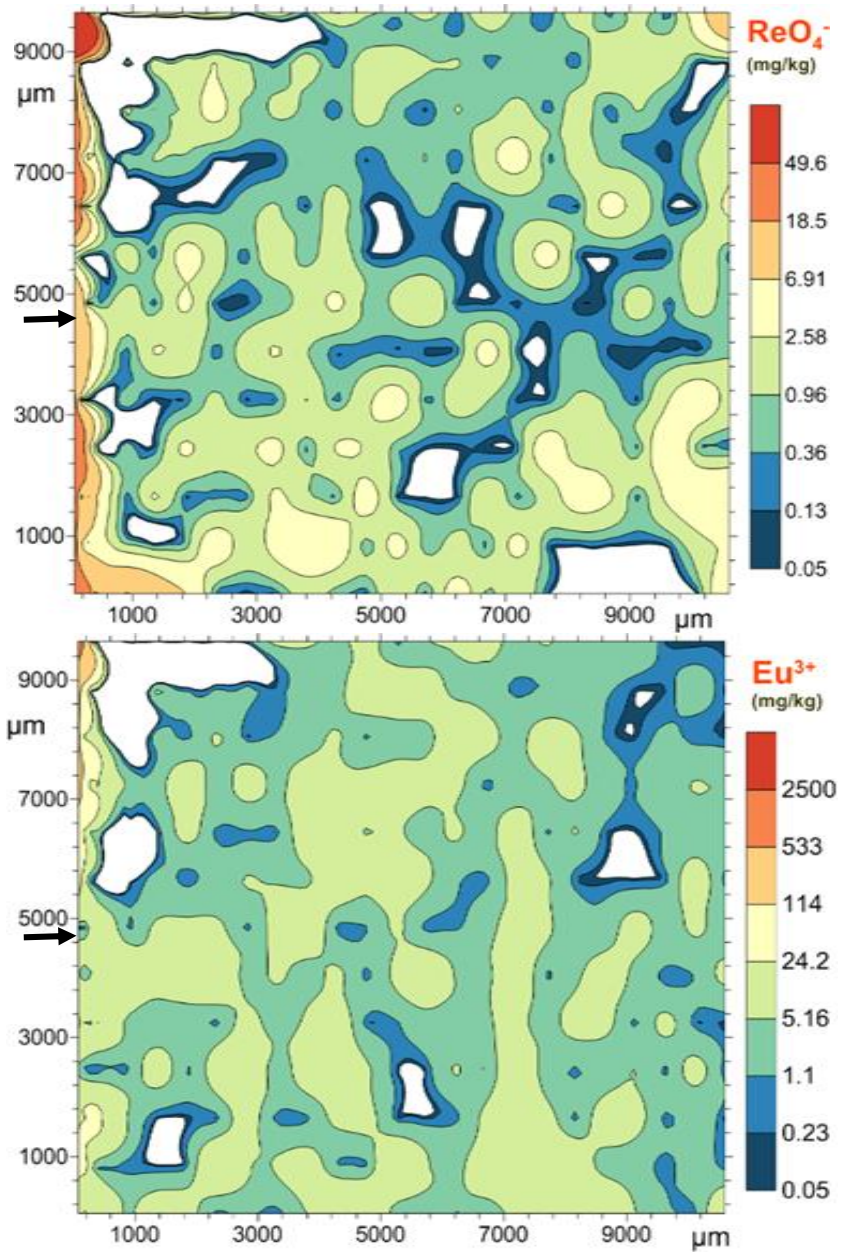

Figure 4-10 Tracer imbibition (Brine) of ND Lower Bakken Member (interior face) using perrhenate and europium ions as tracers; arrows on the left indicate base of sample and direction of tracers' imbibition

4.3 Saturation Diffusion and LA-ICP-MS Analyses

The tracer distribution in shale is then mapped with laser ablation-inductively coupled plasma-mass spectrometry. For two molecular tracers in *n*-decane with the sizes of 1.393 nm × 0.287 nm × 0.178 nm for 1-Iododecane and 1.273 nm × 0.919 nm × 0.785 nm for trichlorooxobis (triphenylphosphine) rhenium (V), much less diffusive penetration was observed for wider molecules of trichlorooxobis (triphenylphosphine) rhenium (V) in oil-wetting shales with median pore-sizes of several nanometers.

The LA-ICP-MS analyses also map tracer distribution patterns from the saturated diffusion experiments (Figure 4.9). The LA–ICP–MS method gives both (1) the rate of decrease in concentration from the edge to some plateau (constant) concentration, and (2) the depth at which the plateau concentration is reached; both are related to the pore connectivity of the matrix.

Observe the trend of tracer distribution from North-East to the south in the Lower Bakken for saturated diffusion (figure 4.12), the pore connectivity trend probably explains the high peak observed in the increasing pore volume from MICP, while the other maps for the other members will be an indicative of the scattered pore distribution in the samples.

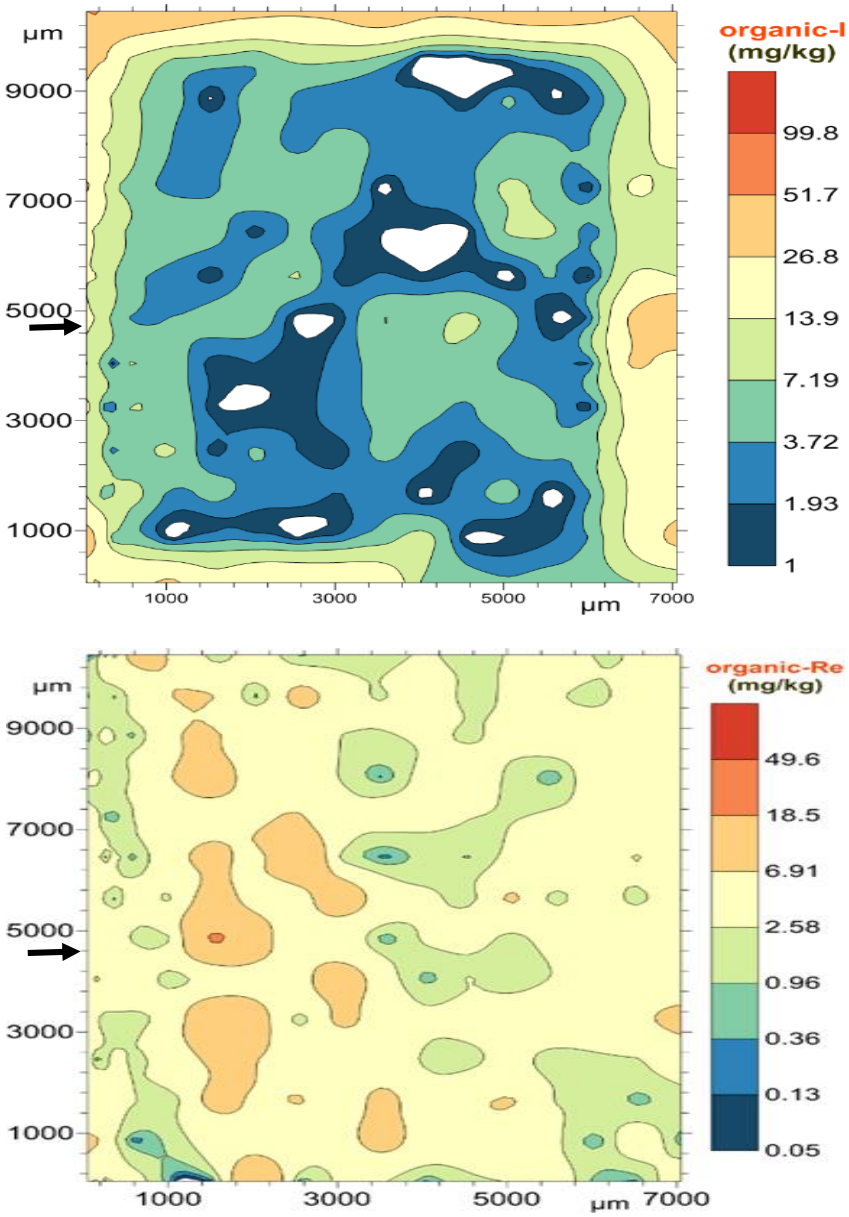

Figure 4-11 Saturated diffusion (Decane) in ND Upper Bakken Member (interior face) using organic-iodine and rhenium (V); arrows on the left indicate base of sample and direction of tracers' diffusion

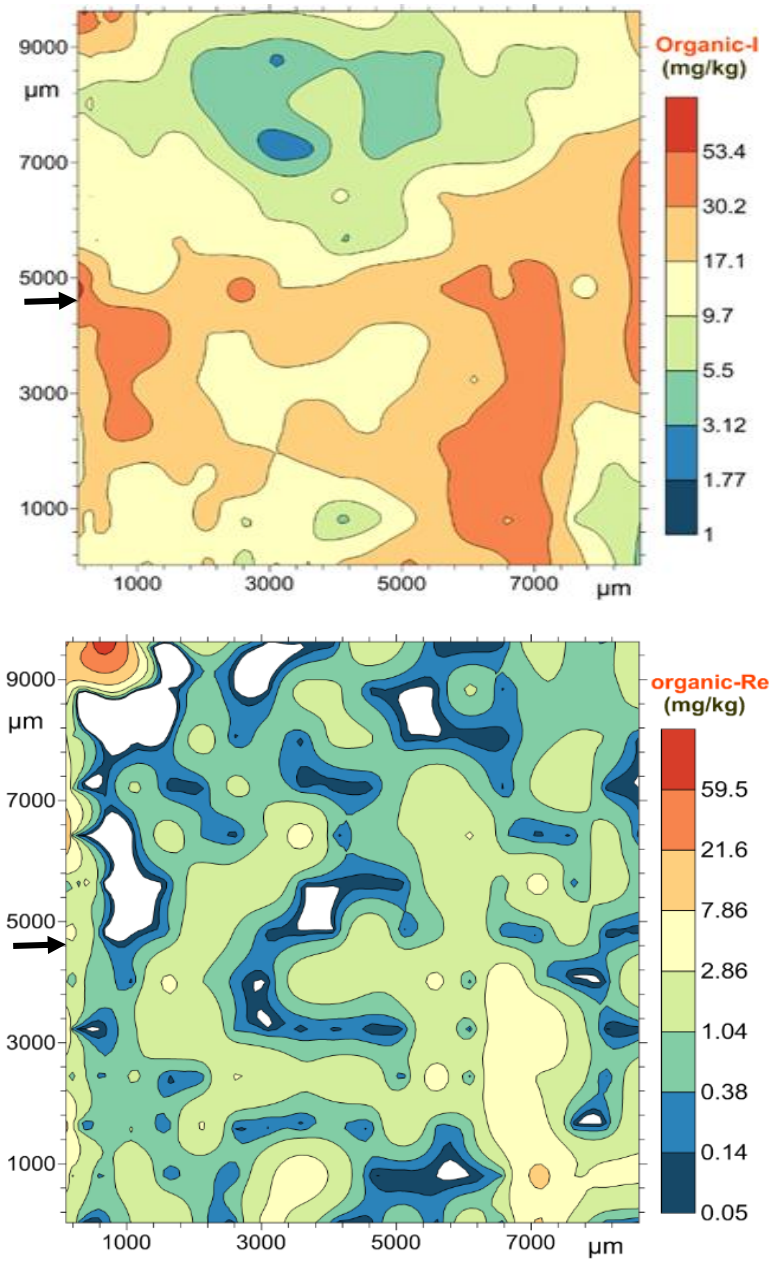

Figure 4-12 Saturated diffusion (Decane) in ND Middle Bakken Member (interior face) using organic-iodine and rhenium (V); arrows on the left indicate base of sample and direction of tracers' diffusion

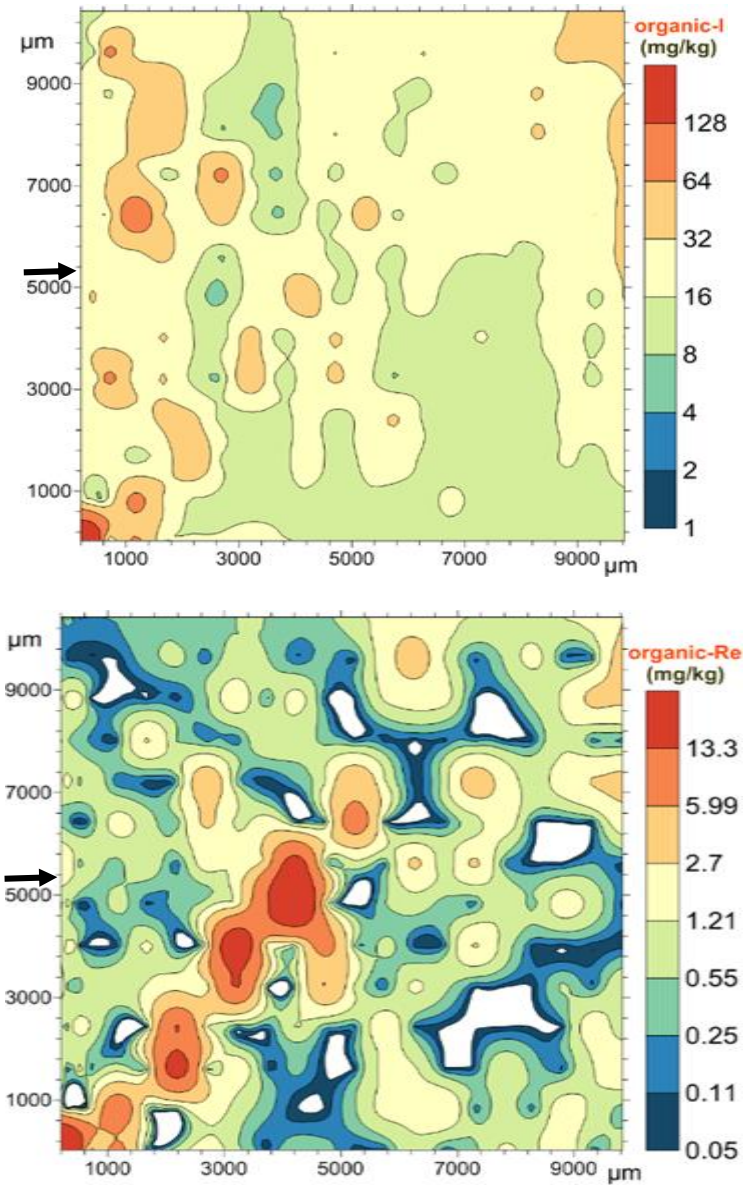

Figure 4-13 Saturated diffusion (Decane) in ND Lower Bakken Member (interior face) using organic-iodine and rhenium (V); arrows on the left indicate base of sample and direction of tracers' diffusion

Chapter 5

Conclusion and Recommendations

5.1 Conclusion

Using different complimentary suites of core-scale analyses and pore-scale network modeling, this project looked into the prevailing low pore connectivity in natural rock that might have originated from lithological and grain-size arrangement (sorting), as well as processes such as burial diagenesis and metamorphism. It is no doubt that the size and geometry of the pores along with and tortuosity of the other connecting throats all have huge effects in the productivity of a reservoir, however, a study of how the effects cut across all tight plays is worth probing.

Results from the MICP indicates that the Bakken pores are predominantly in the nanometer size range, with an average pore-throat diameter of 7.8, 6.8 and 17.6 for the Upper, Middle and Lower Bakken members respectively. The porosity and permeability values measured were also very low in line with the low pore diameters obtained.

The small pore size and low pore connectivity lead to anomalous imbibition behavior, consistent with percolation theory. The calculated imbibition slopes indicates low pore connectivity within the sample used in the test.

The small pore size and low pore connectivity lead to extremely low diffusion rates in the tight matrix, as measured using liquid tracer diffusion approach and LA–ICP–MS mapping. In general, the LA-ICP-MS analyses indicate that only less than 10% of the porosity (especially from the tracer

imbibition) in the middle of a sample is connected to the exterior while the interior tracer concentration and distribution are limited by tortuous pathways. The decrease in concentrations away from the edge pores and base suggest that only small portion of the nanopores in the Bakken samples are connected for diffusion and imbibition. Also much less tracer penetration into samples was observed for the wider molecules, suggesting that the nano-sized molecules become entangled in the Bakken's nanopores.

We find that the Bakken members, and likely other tight plays as well, have very limited edge-accessible pore spaces. This is shown from low pore connectivity behavior of fluid (water brine and *n*-decane) imbibition, and a limited connected pathways of tracers from tracer imbibition and saturation diffusion. This sparse, and limited, pore space connection revealed within the Bakken play will lead to the limited fracture-matrix interactions in fractured shale, and consequently steep initial production decline and overall low recovery.

5.2 Recommendations

The effect of the low pore connectivity and short connected distance that these observations reveal will lead to steep initial decline and low overall production in the Bakken play, hence the need to conduct more studies on pore structure. The results of this project can bridge knowledge gaps in nano-scale pore structure effects on macro-scale fluid migration and behavior in hydraulically stimulated shale formations, which can lead to the development of viable approaches to improving fluid productivity and associated economic benefits of

unconventional resource utilization. More studies should be conducted to further observe pore structure along with fluid behavior and dynamics within the nanopores using other capturing instruments like Small Angle Neutron Scattering (SANS) and Nuclear Magnetic Resonance (NMR) analyses.

From the limited accessibility and connectivity of nanopores in Bakken Formation observed here, we further recommend repositioning of the stimulated hydraulic fractures in the wells to further expose and connect with the isolated and ineffective pores within the matrix for improved and overall oil recovery in the Bakken and other unconventional shale plays.

References

Alexandre, C.S., 2011. Reservoir Characterization and Petrology of the Bakken Formation, Elm Coulee Field, Richland County, MT: *Colorado School of Mines, M.S. Thesis*

Anna, L., Pollastro, R., and Gaswirth, S., 2011. Williston Basin Province-Stratigraphic and Structural framework to a geologic assessment of undiscovered oil and gas resources, *Chap 2 of. f U.S. Geological Survey Williston Basin Province Assessment team, Assessment of undiscovered oil and gas resources of the Williston Basin Province of North Dakota, Montana, and South Dakota, 2010, Volume U.S. Geological Survey Digital Data Series* 69-W, p. 17.

Breit, V.S., Stright Jr. D.H., and Dozzo, J.A., 1992. Reservoir Characterization of the Bakken Shale From Modeling of Horizontal Well Production Interference Data. *SPE Rocky Mountain Regional Meeting held in Casper, Wyoming.*

Cook, T.A., 2013., Procedure for calculating estimated ultimate recoveries of Bakken and Three Forks Formations horizontal wells in the Williston Basin: *U.S. Geological Survey Open-File Report 2013–1109,* 14 p., *http://pubs.usgs.gov/of/2013/1109/.*

Dev K.G., and Hsui A.T., 1987. Origin of Cratonic Basins; *Geology*, *vol. 15,* Issue 12, p.1094.

Energy & Environmental Research Center., 2013. Bakken Formation http://www.undeerc.org/bakken/bakkenformation.aspx

Ewing, R.P., and Horton R., 2002. Diffusion in sparsely connected pore spaces: Temporal and Spatial Scaling. *Water Resour. Res*., 38: 1285, doi:10.1029/2002WR001412.

Gao, Z.Y., and Hu, Q., 2013. Estimating Permeability Using Median Pore-throat Radius Obtained From Mercury Intrusion Porosimetry. *J. Geophy Eng. 10,(*2).

Gerhard, L.C., Anderson, S.B., LeFever, J.A., and Carlson, C.G., 1982. Geological Development, Origin, and Energy Mineral Resources of Williston Basin, North Dakota: *AAPG Bulletin, 66(8):* 989-1020.

Gerhard, L.C., Anderson, S. B., and LeFever, J.A., 1987. Structural history of the Nesson Anticline, in Longman, M. W., ed., Williston Basin: Anatomy of a Cratonic Oil Province: *Rocky Mountain Association of Geologists*, p. 337-353.

Heck, T.J., LeFever, R. D., Fischer, D.W. and LeFever, J., 1999. Overview of the Petroleum Geology of the North Dakota Williston Basin; *Publication of* Department of Mineral Resources, North Dakota Geologic Survey.

Hester, T.C., and Schmoker, J.W., 1985. Selected Physical Properties of the Bakken Formation, North Dakota and Montana Part of the Williston Basin: U.S. Geological Survey Oil and Gas Investigations Chart, OC-126, 1sheet.

Hu, Q., Kneafsey, T.J., Trautz, R.C., and Wang, J.S.Y., 2002. Tracer Penetration into Welded Tuff Matrix from Flowing Fractures. Vadose Zone J., 1: 102–112.

Hu, Q., Ewing, R.P. and Dultz, S., 2012. Pore connectivity in Natural Rock. *J. Contam. Hydrol.*,133: 76–83.

Hu, Q., and Mao, X.L., 2012. Applications of Laser Ablation-Inductively Coupled Plasma-Mass Spectrometry in studying Chemical Diffusion, Sorption, and Transport in Natural Rock. *Geochem. J.,* 46 (5):459–475.

Hu Q., Gao, X. Gao, Z., Ewing, R., Dultz, S., and Kaufmann, J., 2014. Pore Accessibility and Connectivity of Mineral and Kerogen Phases in Shales. *Unconventional Resources Technology Conference (URTeC)*

Hunt, A.G., Ewing, R.P., and Ghanbarian, B., 2014. Percolation Theory for Flow in Porous Media 3rd ed., *Lect. Notes Phys. 880, Springer, Heidelberg.*

Jin, H., and Sonnenberg S.A., 2012. Source Rock Potential of the Bakken Shales in the Williston Basin, *North Dakota and Montana Search and Discovery Article #20156*

Kathleen Neset., 2014. Myths of Bakken: Bismarck Tribune Nov 17th 2014 http://bismarcktribune.com/bakken/breakout/myths-of-the-bakken

Katz, A.J., and Thompson A.H., 1986. A quantitative prediction of permeability in porous rock. *Phys. Rev. B., 34*: 8179–81.

Kuhn, P.P., Primio, R., Hill, R., Lawrence, J.R., and Horsfield, B., 2012. Three-Dimensional Modelling study of the low permeability petroleum system of the Bakken Formation. *AAPG Bulletin*, *v. 96, no. 10,* pp. 1867-1897.

LeFever, J. A., Martiniuk, C.D., Dancsok, E.F.R., and Lund, D.F., 1991. Petroleum Potential of the Middle Member, Bakken Formation, Williston basin, *in* Christopher, J. E. and F. Haidl, eds., *Proceedings of the sixth*

international Williston Basin Symposium: Saskatchewan Geological Society, Special Publication 11, p. 74–94.

LeFever, J. A., 2005. Oil Production from the Bakken Formation: A Short History; *North Dakota Geological Survey Newsletter*, v.32, no.1, p.1-6

LeFever, J.A., 2007b. Lithofacies of the middle Bakken member, North Dakota, *North Dakota Geological Survey Geologic Investigations pdf.*

LeFever, J.A., 2008. Structural contour and isopach maps of the Bakken Formation in North Dakota: *North Dakota Geological Survey Geologic Investigations.*

Li, K., 2007. Scaling of spontaneous imbibition data with wettability included. *J. Contam. Hydrol.*,89: 218–230.

Meissner, F. F., 1978. Petroleum geology of the Bakken Formation, Williston basin, North Dakota and Montana, *in* D. Rehrig, ed. The Economic Geology of the Williston Basin: *Proceedings of the Montana Geological Society*, *24th Annual Conference,* p. 207-227.

Monahan, P. D., 2014. Depositional Facies and Reservoir Analysis of the Tyler Formation in the Central Williston Basin, North Dakota*. M.S. Thesis, University of Texas at Arlington.*

Nelson P. H., 2009. Pore-throat sizes in Sandstones, Tight sandstones, and Shale *AAPG Bulletin, 93 (3):* 329– 340

North Dakota Drilling & Production Statistics; Historical monthly; Bakken Oil Production Statistics, September 2013. *https://www.dmr.nd.gov/oilgas/stats/statisticsvw.asp*

Olafuyi, O.A., Cinar, Y., Knackstedt, M. A., and Pinczewski, W.V., 2007. Spontaneous Imbibition in Small Cores Bakken Shale. *SPE 109724*. Presented at the SPE Asia Pacific Oil &Gas Conference Oct. - Nov. 2007

Olesen, N.L., 2010. Bakken Oil Resource Play, Williston Basin (US), Overview and Historical Perspective; Continental Resources.

Peng, S., Hu, Q., Ewing, R.P., Liu, C., and Zachara, J.M., 2012. Quantitative 3-D Elemental Mapping By LA-ICP-MS of Basalt from The Hanford 300 Area. *Environ. Sci. Technol.*, 46: 2035–2042.

Pitman, J.K., Price, L.C., and LeFever, J.A., 2001*. Diagenesis and Fracture* Development in the Bakken Formation, Williston Basin—Implications for Reservoir Quality in the Middle Member. U.S. Geological Survey Professional Paper 1653.

Pollastro, R.M., Roberts, L.N.R., and Cook, T.A., 2010. Geologic Assessment of Technically recoverable oil in the Devonian and Mississippian Bakken Formation, Chap. 5 of U.S. Geological Survey Williston Basin Province Assessment Team, Assessment of undiscovered oil and gas resources of the Williston Basin Province of North Dakota, Montana, and South Dakota, 2010 (ver. 1.1, November 2013): U.S. Geological Survey Digital Data Series DDS–69–W, 34 p

Price, L. C., and LeFever, J., 1994. Dysfunctionalism in the Williston Basin: The Bakken/Mid-Madison petroleum system: *Bull. Canadian Petrol. Geol.,* 42: 187-218.

Ramakrishna S., Balliet, R., Miller, D., Sarvotham, S., and Merkel, D., 2010. Formation Evaluation in the Bakken Complex Using Laboratory Core Data and Advanced Logging Technologies. *SPWLA 51st Annual Logging Symposium.*

Sarg, F.J., 2012. The Bakken - An Unconventional Petroleum and Reservoir System; *Final Scientific Report, Colorado School of Mines DOE Award No.: DE-NT0005672.*

Shahri, M.P., Jamialahmadi, M., and Shadizadeh, S.R., 2012. New Normalization Index for Spontaneous Imbibition. *J. Petrol. Sci. Eng.*, 82-83: 130–139.

Shuler P., Tang H., Lu Z., and Tang Y., 2011. Chemical Processes for Improved Oil Recovery From Bakken Shale. *CSUG/SPE* 147531. *Presented at the Canadian Unconventional Resources Conference, Calgary, Canada. November 2011.*

Simenson, A., 2010. Depositional Facies and Petrophysical Analysis of the Bakken Formation, Parshall Field, Mountrail County, North Dakota. *Colorado School of Mines, M.S. Thesis.*

Sloss, L. L., 1963. Sequences in the Cratonic Interior of the North America: *GSA Bull., 74*, 93-114.

Smith, M.G., and Bustin, R.M., 1995. Sedimentology of the Late Devonian and Early Mississippian Bakken Formation, Williston Basin, in Seventh International Williston Basin Symposium Guidebook: *Billings, Montana Geological Society,* p. 103–114.

Sonnenberg, S. A., 2014. Upper Bakken Shale Resource Play, Williston Basin *Search and Discovery Article #10625*

Standnes, D., and Austad, T., 2000. Wettability Alteration in Chalk 2. Mechanism for Wettability Alteration from Oil-Wet to Water-Wet Using Surfactants. *J. Petrol. Sci. and Eng*. 28:, 123-143

Standnes, D.C., 2010. Scaling spontaneous imbibition of water data accounting for fluid Viscosities. *J. Petrol. Sci. Eng.,* 73: 214–219.

Tiab, D., and Donaldson, E., 2012. Theory and Practice of Measuring Reservoir Rock and Fluid Transport Properties. *Gulf Professional Publishing*.

Tran T., 2011. Bakken Shale Oil Production Trends; *Texas A&M University, M.S. Thesis*

US Department of the Interior., 2013. USGS Releases of New Oil and Gas Assessment for Bakken and Three Forks, 30 Apr. 2013.

Wang, D., Butler, R., Liu, H., and Ahmed, S., 2010. Flowrate Behavior and Imbibition in Shale. *SPE 138521. Presented at the SPE regional meeting in West Virginia, October 2010.*

Wang, D., Butler, R., Zhang, J., and Seright, R,. 2012. Wettability Survey in Bakken Shale with Surfactant-formulation Imbibition, *SPE Reserv. Eval. Eng. 15(6),* 695-705

Biographical Information

Joseph Ikechukwu Anyanwu is the third of seven children of Mr. and Mrs. A.E. Anyanwu. He graduated with Bachelor of Technology from the Federal University of Technology, Owerri, in Imo State, Nigeria in 2006, and a Master's of Science in Geology from the University of Texas at Arlington in 2015. His undergraduate research was in Sedimentology and particle size distribution and this led him to choose the petroleum geology option for his graduate program. While at the University of Texas at Arlington, his research interest was in petrophysics and low-pore connectivity in unconventional resource plays, hence a focus on nanopetrophysics of Bakken play. After graduation, Joseph intend to work and build a career in the oil and gas industry.